



RESISTIVITY AND MAGNETORESISTIVITY OF FINE
INDIUM WIRES AT LOW TEMPERATURES

Thesis for the Degree of M. S.
MICHIGAN STATE UNIVERSITY
Alan Fredrick Burmester
1965

THESIS

C.2



MICHIGAN STATE UNIVERSITY
DEPARTMENT OF PHYSICS
EAST LANSING, MICHIGAN

PLACE IN RETURN BOX
to remove this checkout from your record.
TO AVOID FINES return on or before date due.

DATE DUE	DATE DUE	DATE DUE
<hr/>	<hr/>	<hr/>
<hr/>	<hr/>	<hr/>
<hr/>	<hr/>	<hr/>
<hr/>	<hr/>	<hr/>
<hr/>	<hr/>	<hr/>

ABSTRACT

RESISTIVITY AND MAGNETORESISTIVITY OF FINE INDIUM WIRES AT LOW TEMPERATURES

by Alan Fredrick Burmester

When one of the physical dimensions of a conductor approaches the mean free path length of the charge carriers, the observed resistivity of the conductor is increased over the value found for the bulk material. This increase in resistivity is known as the electrical resistance size effect. The mechanism of this effect is the introduction of surface scattering as a relaxation mechanism which is comparable to impurity and phonon scattering

This size effect in thin films has recently been the object of much experimental and theoretical investigation. However, thin wires have not seen so much attention probably due to the more complex geometry and sample production problems.

This investigation has been concerned with the electrical resistance size effect in indium wires ranging in diameter to a lower limit of .0156mm. The temperature dependence of the effect was observed between 4.2°K and 1.1°K. Magnetoresistive size effects were observed in fields up to 20 kilogauss.

The increase in resistivity with decreasing size observed in this work agrees well with work done previously on larger wires. A maximum in the magnetoresistance of some of the smaller wires was observed. A simple calculation

Alan F. Burmester

based on this maximum and the size dependence of the increased resistivity lead to values of 1.0×10^{-19} gm-cm/sec for charge carrier momentum and a concentration of .4 carriers per atom.

**RESISTIVITY AND MAGNETORESISTIVITY OF FINE
INDIUM WIRES AT LOW TEMPERATURES**

By

Alan Fredrick Burnester

A THESIS

**Submitted to
Michigan State University
in partial fulfillment for the requirements
for the degree of**

MASTER OF SCIENCE

Department of Physics and Astronomy

1965

4258
-14-65

ACKNOWLEDGMENTS

It is my pleasure to express my sincere appreciation to Dr. F. J. Blatt who suggested the problem and offered continued aid and encouragement throughout the course of the work.

The guidance of Dr. M. Garber in some of the experimental details and interpretation of the data is also acknowledged.

I am grateful to the Atomic Energy Commission for financial support of this work.

TABLE OF CONTENTS

Chapter		Page
I	Introduction	1
II.	Theoretical.	4
III.	Experimental Arrangement and Procedures.	13
IV.	Presentation of Data and Discussion of Results.	25
V.	Conclusions.	55
	References	58

LIST OF FIGURES

Figure		Page
1.	The Sample Extrusion Apparatus	13
2.	The Sample Holder.	16
3.	The Measuring Circuit.	22
4.	Resistivity vs. Magnetic Field; Sample III-1 . .	27
5.	Resistivity vs. Magnetic Field; Sample III-5 . .	28
6.	Resistivity vs. Magnetic Field; Sample VI-2. . .	29
7.	Resistivity vs. Magnetic Field; Sample III-6 . .	30
8.	Resistivity vs. Magnetic Field; Sample IV-6. . .	31
9.	Resistivity vs. Magnetic Field Squared; Sample III-1.	34
10.	Resistivity vs. Magnetic Field Squared; Sample III-5.	35
11.	Resistivity vs. Magnetic Field Squared; Sample III-6.	36
12.	Resistivity vs. Magnetic Field Squared; Sample IV-6	37
13.	Kohler Plot for Sample III-1	39
14.	Kohler Plot for Sample IV-2.	40
15.	Kohler Plot for Sample IV-5.	41
16.	Kohler Plot for Sample IV-6.	42
17.	Kohler Plot for Various Samples at 4.2°K	46
18.	Kohler Plot for Various Samples at 2.5°K	47
19.	Resistivity vs. Reciprocal Diameter at 4.2°K . .	49
20.	Resistivity vs. Reciprocal Diameter at 0°K . . .	52
21.	Phonon-Surface Resistivity vs. $\left(\frac{d}{2}\right)^3$ at 4.2°K. .	53

LIST OF TABLES

Table		Page
I	Description of Samples	26
II	Tabulation of Resistivities in Zero Magnetic Field at Various Temperatures .	44

Chapter I

Introduction

At room temperatures the electrical resistivity of a metallic conductor is independent of the shape or size of the material. However, at low temperatures it has been observed that material which has been formed into thin films or wires has a higher resistivity than the bulk material at the same temperature. This effect, known as the resistance size effect, is due to diffuse scattering of the conducting charge carrier at the surface. The effect becomes observable only when the mean free path of these carriers is comparable to the smallest dimension of the conductor.

This size effect was first observed in thin silver films by Stone in 1899 (1), and was treated theoretically by J. J. Thompson in 1901 (2). With the introduction of liquid helium research techniques and the availability of ultra pure metals, studies can be conducted in the range where the mean free path is much greater than the sample dimension. Under these conditions the size dependence of the resistivity is a major effect. A good approximation for the increased resistivity due to this effect in a cylindrical wire is given by the expression $\rho_b + \frac{\alpha \rho_b l}{d}$, where ρ_b is the bulk resistivity, l the mean free path in the bulk, d the diameter of the wire, and α a geometrical factor which is close to unity (3). Measurements of resistivity as a function of wire diameter enable a determination of ρ_b and l to be made. More importantly, the

product $\rho_b l$ which is directly determined is a measure of the momentum of the carriers at the Fermi surface.

Closely related to the above effect is a size dependence of the magnetoresistance in thin films and wires. This effect has been treated theoretically for thin films (4,5) and for wires in a longitudinal field (6). A successful theory is yet to be developed for thin wires in a transverse field. Size effect experiments of this type may lead to some information regarding the momentum of electrons at the Fermi surface.

Consideration of a temperature dependent size effect in zero magnetic field may give some information regarding the nature of the resistivity of the bulk metal at very low temperature.

The present paper is an extension of the experimental work of J. L. Olsen (7) to indium wires smaller in size by about one order of magnitude and in magnetic fields approximately twice as great. Preliminary work on this problem was done by B. C. LaRoy (8) and a good review of the literature on this subject prior to 1963 appears in his work.

Indium is a good material for these studies because its bulk magnetoresistance saturates at a field well within the available range. It was hoped that this would facilitate the separation of the various size effects in the magnetic field. From a practical point of view, indium can be extruded to very fine diameters (~ 0.01 mm); furthermore it

anneals at room temperature. It is also commercially available in a high state of purity.

The resistivities referred to herein are a function of both applied magnetic field and temperature and will be symbolized by $\rho(H,T)$. A subscript is used to indicate whether the symbol refers to the sample resistivity $\rho_w(H,T)$, or to the bulk resistivity $\rho_b(H,T)$.

Chapter II

Theoretical

Bulk Resistivity

The expression for electrical resistivity of a metal according to the free electron model of metals is

$$\rho = \frac{m}{Ne^2\tau} \quad (1)$$

Here N is the number of free electrons per unit volume and is given by the number of atoms per unit volume times the number of free electrons per atom, τ is a characteristic relaxation time which is the average time of travel of the electrons between scattering events, e is the electron charge and m is its mass. The free electron model neglects the interaction of the electrons with the lattice potential. As a first approximation, the effect of this potential may be taken into account by replacing m with an effective mass m^* which compensates for the effect of the periodic lattice potential on the electron.

Since electrons obey the Pauli Exclusion Principle Fermi-Dirac statistics must be applied. In a metal at low temperature these statistics lead to a highly degenerate distribution. Thus only electrons with energies near the Fermi level having Fermi velocity V_f participate in the charge transport. The Fermi velocity is given by

$$V_f = \left[\frac{2E_f}{m^*} \right]^{\frac{1}{2}} \quad (2)$$

where E_f is the Fermi Energy. We now define the mean free path by $l = V_f \tau$. Thus

$$\rho = \frac{m^* V_f}{Ne^2 l} = \frac{P_f}{Ne^2 l} \quad (3)$$

where P_f is the Fermi momentum. The above discussion assumes one group of charge carrier with isotropic effective mass, a situation which is rarely encountered in practice. A better approximation to a real metal is often made by assuming a current which is presumed to arise from the motion of two types of charge carriers having differing isotropic effective mass, number density and possibly electric charge. This is known as the two band model.

If the scattering of electrons is accomplished by several mechanisms acting independently, a characteristic relaxation time may be associated with each. Then the effective relaxation time is

$$\frac{1}{\tau_{eff}} = \frac{1}{\tau_1} + \frac{1}{\tau_2} + \dots \quad \text{and} \quad \frac{1}{l_{eff}} = \frac{1}{l_1} + \frac{1}{l_2} + \dots \quad (4)$$

In this case resistivities due to each separate mechanism are additive and we arrive at Matthiessens Rule

$$\rho_{eff} = \frac{P_f}{Ne^2} \left(\frac{1}{l_1} + \frac{1}{l_2} + \dots \right) = \rho_1 + \rho_2 + \dots \quad (5)$$

In bulk metals the usual form of Matthiessen's rule is obtained by identifying two scattering mechanisms. Lattice imperfections such as impurities and dislocations contribute a temperature independent term while thermally

excited lattice vibrations (phonons) produce a temperature dependent term. Equation (5) is then

$$\rho_b(T) = \frac{P_f}{Ne^2} \left(\frac{1}{l_i} + \frac{1}{l_p(T)} \right) \quad (6)$$

or
$$\rho_b(T) = \rho_i + \rho_p(T)$$

where ρ_i is the resistivity due to impurity scattering and other temperature independent effects and $\rho_p(T)$ is the resistivity due to phonon scattering.

Temperature Independent Size Effect

If the conductor has physical dimension comparable to the mean free path in the bulk then the charge carriers will be scattered by the surface of the specimen an appreciable portion of the time. If this surface scattering is independent of the other scattering mechanisms, then applying Matthiessen's rule:

$$\rho = \frac{P_f}{Ne^2} \left(\frac{1}{l_b} + \frac{1}{l_s} \right) \quad (7)$$

where l_b is the effective mean free path in the bulk material and l_s is the mean free path associated with surface scattering. Identifying l_s with a physical dimension such as the diameter of a wire, we have the expression derived by Nordheim (3):

$$\rho_w = \rho_b \left(1 + \frac{\alpha l_b}{d} \right) \quad (8)$$

where α is a coefficient which expresses the nature of the

surface scattering, ranging from zero, for specular scattering to unity in the case of diffuse scattering. Observations indicate that for most metals the surface scattering is entirely diffuse (9, 10). More sophisticated treatments based on the solution of the Boltzman equation have been published by Fuchs (11) for thin films and Dingle (12) for thin wires. Calculations by Sondheimer (9) based on Dingle's theory agree to within 5% with results of the Nordheim equation.

On the basis of equation (8) the temperature dependent part of the resistivity should be independent of the wire size. However, the results of an experiment by Olsen (7) indicated that the temperature dependence of the resistivity of thin indium wires is greater than that of the bulk material. The following explanation suggested by Olsen has been expanded by Blatt and Satz (13) and has been investigated with computer methods by Luthi and Wyder (14).

The maximum angle through which an electron can be deflected by phonon scattering is

$$\theta_{\max} \approx \frac{\text{momentum of phonon}}{\text{momentum of electron}} \approx \frac{T}{\theta_D} \frac{K_D}{k_F} \quad (9)$$

where K_D is the wave vector of a phonon of energy $k\theta_D$, k_F is the wave vector of an electron at the Fermi surface and θ_D is the Debye temperature. For metals $K_D/k_F \sim 1$ so that at low temperatures ($T \ll \theta_D$) the angle through which electrons are scattered thermally is very small $\sim (T/\theta_D)$.

Hence, in the bulk material many thermal collisions are required to remove the forward momentum of an electron traveling parallel to the axis of the wire. However, in the case of a small wire even a small deflection due to phonon scattering may suffice to bring the electron to the surface where it is scattered diffusely. Thus with decreasing size, phonon scattering becomes an ever more effective relaxation mechanism.

Blatt and Satz assume that

$$\rho_w = \rho_i + \rho_p + \rho_s + \rho_{ps} \quad (10)$$

where ρ_{ps} is the increase in resistivity due to the above phonon-surface mechanism. They derived the following expression for ρ_{ps}

$$\rho_{ps} = \left(2\pi \rho_b^2 l^2 \right)^{\frac{1}{3}} \left(T/\theta_D \right)^{\frac{2}{3}} (\rho_b)^{\frac{1}{3}} \left(\frac{d}{2} \right)^{-\frac{2}{3}} \quad (11)$$

Subject to the following assumptions:

- a. $l \gg d$
- b. $T \ll \theta_D$
- c. The differential scattering cross section is a constant for the allowed scattering angles.
- d. Umklapp scattering is neglected.

When compared with the results of Olsen (7) on indium and Andrew (10) on mercury, the predicted value of ρ_{ps} is consistently too high. This may be due to the fact that the measured value of ρ_b which enters in the above equation contains the resistivity due to both Normal and Umklapp scattering whereas the derivation of the expression for ρ_{ps}

neglected Umklapp events. By dividing ρ_b by a suitable constant such that predicted values of ρ_{ps} agree with observed values, the ratio of Normal to Umklapp resistivities may be estimated.

Magnetic Effects

If a conductor which is carrying a current is placed in a magnetic field, the Lorentz force on the current carriers will force them into curved orbits. In a metal which has only one type of carrier this curvature deflects all carriers to one side of the conductor which in turn creates a Hall electric field. This field will then just counteract the Lorentz forces on the carrier producing an undeviated path. To explain magnetoresistance then, one must consider a two band model. In this case the two forces do not cancel and the carriers are deflected into orbits giving rise to an increase in resistance. It may be expected that the effect of the applied field on the resistance of the conductor will depend upon the radius of the orbit (r_c) compared to the mean free path of the carriers. From

$$(H) \left(\frac{1}{\rho_{(0,T)}} \right) = \left(\frac{cP}{er_c} \right) \left(\frac{Ne^2 \ell}{P_f} \right) = (Nec) \frac{\ell}{r_c} \quad (12)$$

we see that $H/\rho_{(0,T)}$ is a measure of the dimensionless parameter ℓ/r_c . Consequently, in discussing the effect of the magnetic field, $H/\rho_{(0,T)}$ is used as the independent variable (15).

In particular it can be shown that

$$\frac{\Delta\rho}{\rho_b(0,T)} = f\left(\frac{H}{\rho_b(0,T)}\right) \quad (13)$$

In this relation, known as Kohler's rule, $\rho_b(0,T)$ is the zero field resistivity, $\Delta\rho$ is the change in the resistivity in the applied field H and f is a function of $\frac{H}{\rho_b(0,T)}$ which is characteristic of the particular metal and independent of temperature. A specific example of this general rule is an expression derived by Sondheimer and Wilson (16) for the two band model

$$\frac{\Delta\rho}{\rho(0,T)} = \frac{AH^2}{1+BH^2} \quad (14)$$

Here A and B are constant characteristics of the metal. In practice it has been observed that although this expression correctly predicts the occurrence of saturation in indium the transition from the quadratic to the saturation region is actually much broader than predicted by equation (14). Moreover the dependence of the magnetoresistance on applied field at low fields is observed to be somewhat less than quadratic.

The magnetoresistive size effect has been calculated for a thin wire in a longitudinal field by Chambers (6). Olsen has applied his arguments in a qualitative way to the case of thin wires in a transverse magnetic field. He has pointed out that in applying Kohler's rule to thin wires, one should replace the $\rho_b(0,T)$ value by $\rho_w(0,T)$ as measured for that particular wire if the same function $f\left(\frac{H}{\rho}\right)$ is used independent of wire size. With this modification one would expect Kohler's rule to be obeyed under

the weak magnetic field condition where $r_c > d$.

Olsen (7) and LaRoy (8) have observed this to be true at moderate fields. At fields such that $r_c < d$ and with $d \ll l$ they observed that the saturation value of $\frac{\Delta\rho}{\rho_w(0,T)}$ was lower than the value for large wires. Olsen suggested that as the magnetic field is increased and $r_c < d$ the conditions in the wire with respect to surface scattering approach those present in the bulk material and $\rho_w(0,T)$ should therefore be replaced by $\rho_b(0,T)$ in the limit of very strong fields. In other words Kohler's rule must be written

$$\frac{\rho_w(H,T) - \rho_x}{\rho_x} = f\left(\frac{H}{\rho_x}\right) \quad (15)$$

where $\rho_x \rightarrow \rho_b(0,T)$ for strong fields ($r_c \ll d$) and $\rho_x \rightarrow \rho_w(0,T)$ for weak fields ($r_c \gg d$). That is, ρ_x is itself a function of magnetic fields.

Chambers in his calculation of the magnetoresistance of a thin wire in a longitudinal field computes ρ_x for various l/d and l/r_c values. No such tabulation exists for the transverse case. One may still construct a Kohler plot based on the measured $\rho_w(0,T)$ and from observation of departure of this Kohler plot from that of the bulk material one can estimate $r_c(H)$ and hence the Fermi momentum using

$$p_f = \frac{eHr_c}{c} \quad (16)$$

A maximum in magnetoresistance with a subsequent decrease with increasing transverse fields in thin sodium

wires has been observed by McDonald and Sarginson (5). This effect was explained theoretically (5) for thin films with a magnetic field in the plane of the film and for a thin wire of square cross section in a transverse field. The origin of this size dependent effect is the reduction of the surface scattering resistivity which occurs when the cyclotron orbits of the conduction electrons become smaller than the dimensions of the conductor. The electrons traveling in these small orbits are confined to trajectories which meet the surface less often than the trajectories associated with the $r_c > \frac{d}{2}$ condition. The position of this maximum occurs at a field strength such that $r_c \approx \frac{d}{2}$. From the expression for the cyclotron radius P_f may be evaluated. Sondheimer (4) has predicted that the magnetoresistance of a thin film in a magnetic field normal to the plane of the film would be an oscillatory function of the applied field. Both of these effects have recently been observed in thin aluminum and indium sheets by Forsvoll and Holwech (17,18). Previously Babiskin and Siebenmann (19) had observed an oscillatory magnetoresistance in thin sodium wires.

While the theory of magnetoresistance in thin films has been well developed and supported by experimental results, the same can not be said for the case of thin wires. Nevertheless, qualitative remarks which have been made here are probably correct and will provide a background and basis of comparison for the present work.

Chapter III

Experimental Arrangement and Procedures

Sample Preparation

Wire samples were extruded from $\frac{1}{4}$ inch indium rods supplied by American Smelting and Refining Company. The purity of this material was given as 99.999% by the processor.

The extrusion press consisted of a steel cylinder 1" OD x $\frac{1}{4}$ " ID x 3" long to one end of which a diamond die was bolted. A short length of the indium, as supplied, was placed into this cylinder. Pressure was applied from a bench press and hydraulic jack by a $\frac{1}{4}$ " steel piston.

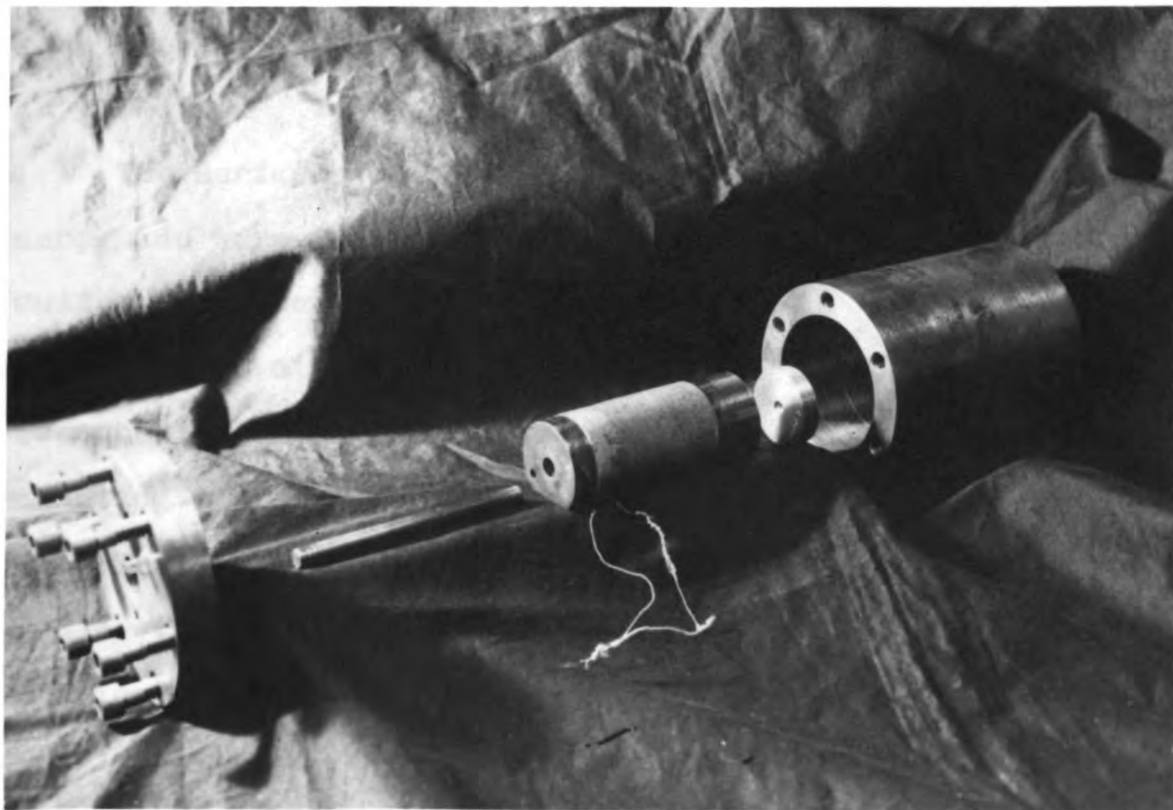


Figure 1 The Sample Extrusion Apparatus

A heater of manganin wire was wound around the extrusion cylinder. It was found, that for die sizes smaller than .003 inches, smoothest wire surfaces were formed when the indium was heated to a temperature of about 120°C. Higher temperatures produced wire which had a beaded appearance while lower temperatures required pressures which placed a severe stress on the steel punch. For the larger size dies heating was not necessary.

The speed of extrusion was found to be important in the formation of wire with smooth surfaces. A formation speed of about 10 centimeters per minute seemed to be the best for the smaller dies. Faster speeds produced twisting and jumping in the formation. A light weight was attached to the end of the smaller wires during the extrusion process to prevent twisting and excessive vibration in the wire.

The surfaces of the wires were examined with a microscope and were found to be of generally regular shape and uniform diameter (variations less than 10%) with occasional scratches or nicks in the surface. The wires were allowed to anneal at room temperature for at least 48 hours after mounting and before being cooled in the resistivity cryostat.

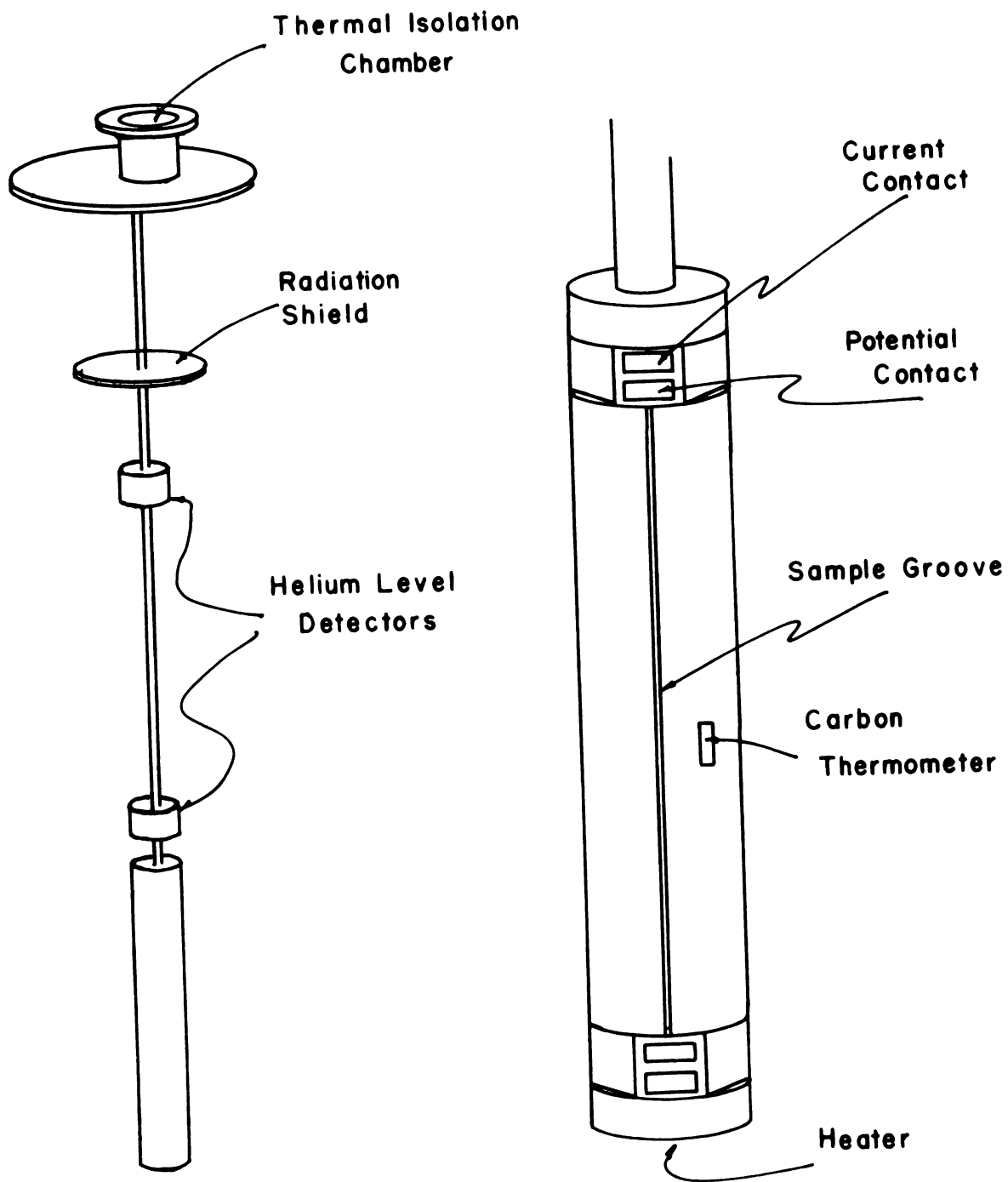
The smallest wire produced by these methods came from a die with a bore of .0005 inch (.013mm). However, due to difficulties encountered in handling and mounting, the smallest wire for which resistivity was successfully measured was from the .0007 (.018mm) inch die.

The diameter of the wire was determined by measuring the resistance of the samples R , in a kerosene bath at room temperature. At this temperature the mean free paths of the electrons due to phonon scattering are small ($\sim 10^{-6}$ cm) compared to the diameter of the smallest specimen; hence the resistivity of the material in the wire should not be a function of its size, and every wire is considered a bulk specimen. The diameter is then given simply by $d = \frac{4\rho L}{\pi R}$. The resistivity, ρ of indium was taken as 8.8×10^6 ohms-cm. at 296°K from White and Woods (20). The length, L , of the wire between the pair of potential contacts in the sample holder was measured with a traveling microscope. In the case of the larger samples, sections which had been taken from the same wire as the experimental sample were also examined and measured by microscope. The two values for the diameter usually agreed to within 2 or 3 percent. The optical measurement was not possible for wires smaller than about .04mm due to diffraction fringes which obscured the edge of the wire.

The Sample Holder

For the resistance measurements the samples were placed in a sample holder which consisted of a one inch diameter glass filled epoxy (glastic) rod 10 inches long. Six separate grooves were cut along the length of the rod. The grooves were .05 inch deep and .02 inch wide. The glastic material was selected for the mounting form because

Figure 2. The Sample Holder



its thermal expansion coefficient closely matched that of the indium samples. Another advantage was that the material was easily machined. Flat surfaces were milled in the rod at each end of the six grooves. At each of these flat surfaces two $\frac{1}{4}$ " x $\frac{3}{16}$ " x $\frac{1}{32}$ " copper blocks were attached by means of epoxy cement. The blocks at the extreme ends of the rod served as current contacts. The potential contact was made by a narrow strip of platinum foil which was soldered to the block nearest to the center of the rod. The platinum was placed in such a manner that the area of contact to the sample was a minimum. This was done to localize the point of contact and to minimize rectifying contacts and contact potentials. The sample length between the contacts was about 20mm.

The six sample wires were connected in series. This connection permitted monitoring the measuring current in all of the samples at once. However, a common measuring current proved inconvenient since the resistances of a set of samples usually differed by about two orders of magnitude making different measuring currents desirable. Moreover, with this type of current connection, when individual samples broke or became disconnected during a measurement run, the entire operation had to be discontinued. For the last set of samples these disadvantages were eliminated by mounting only two samples and rewiring the sample holder with separate current leads for each sample.

The electrical leads for the measuring circuits were

placed in the inside of the sample holder support tube, passed through a wax seal in the dewar cover plate, and terminated in an 18 pin connector. This connector was placed inside of a brass thermal shield for the purpose of minimizing thermal emf in the potential leads.

Sample Mounting

After annealing, the wire sample was placed into the groove in the glastic sample holder in physical contact with the four electrical contact blocks. These contacts were previously tinned with an indium 33 wt. bismuth alloy which melts at 70°C . A small drop of Superior #30 flux was placed at the four connections. Besides aiding in the soldering process, the surface tension of the flux helped to maintain close physical contact between the wire and the contact blocks. A small soldering iron heated to approximately 100°C was placed on the contact block as far away from the sample as possible. The iron was removed just as the solder under the sample melted. In this way contamination of the sample through alloying was reduced to a minimum. The entire length of the groove containing the sample was then filled with a warm glycerin soap solution which jelled at room temperature thus immobilizing the specimen. It was found that if this procedure was not used the Lorentz force due to the magnetic field was sufficient to cause deformation of the sample with an accompanying rise in resistance. In fact some of the

smaller wires were actually broken by Lorentz forces when they had not been supported by this means.

The Cryostat

Temperatures in the 4.2°K to 1.15°K range were obtained by placing the sample holder with liquid helium in a conventional glass double dewar with a narrow tail section. The sample holder was suspended from the dewar cover plate by means of a $\frac{3}{8}$ inch stainless steel tube. Attached to the support tube were two liquid helium level detectors, one just above the sample holder and the other just below the level of the top of the inner vacuum jacket. A copper radiation shield was positioned about 4 inches above the upper level detector. The level detectors consisted of 10 feet of .005 inch tantalum wire wound on a one inch glastic form. The coils had a normal resistance at the superconducting transition temperature of 0.3 ohms. The level of the liquid helium was detected by observing the superconducting resistance transition in the tantalum. In order to prevent the coil from being cooled below the transition temperature (4.3°K) by the cold helium gas during transfer a 30 ohm manganin heater dissipating 100 milliwatts was wound over the tantalum coil and connected in series with it. The general arrangement is shown in figure 2.

Temperatures below 4.2°K were obtained by reducing the pressure at the surface of the helium bath. In order

to insure that the bath was in equilibrium with its vapor at temperatures above the lambda point, 100 milliwatts were dissipated in a 600 ohm heater which was attached to the bottom end of the sample holder. -

For the first two runs (III and IV) the vapor pressure was regulated in the 4.2°K to 2.5°K range by use of a cartesian manostat. For temperatures lower than 2.5°K the manostat had insufficient pumping capacity and it was necessary to use a one inch needle valve in parallel with the manostat to achieve lower temperatures. For the last two runs (V and VI) a Walker regulator (21) with $1\frac{1}{2}$ inch pumping lines was installed. This regulator held the pressure constant to within one part in 10^4 in the range from 760mm to 6mm (1.2°K). Below 6mm it was necessary to pump directly through a two inch valve.

The vapor pressure was measured by a mercury manometer, an oil manometer, or a Macleod gauge depending upon the pressure involved. From this, the temperature in the cryostat was determined by referring to the 1958 Helium Temperature Scale.

An 87 ohm, $\frac{1}{10}$ watt carbon resistor was attached to the sample holder in order to monitor the temperature of the samples. The resistance of this thermometer which had a value of 1,285 ohms at 4.2°K , was measured with a simple D.C. bridge using a Leeds & Northrup type 9834 electronic null detector. With this combination it was possible to determine the temperature to one part in 10^4 .

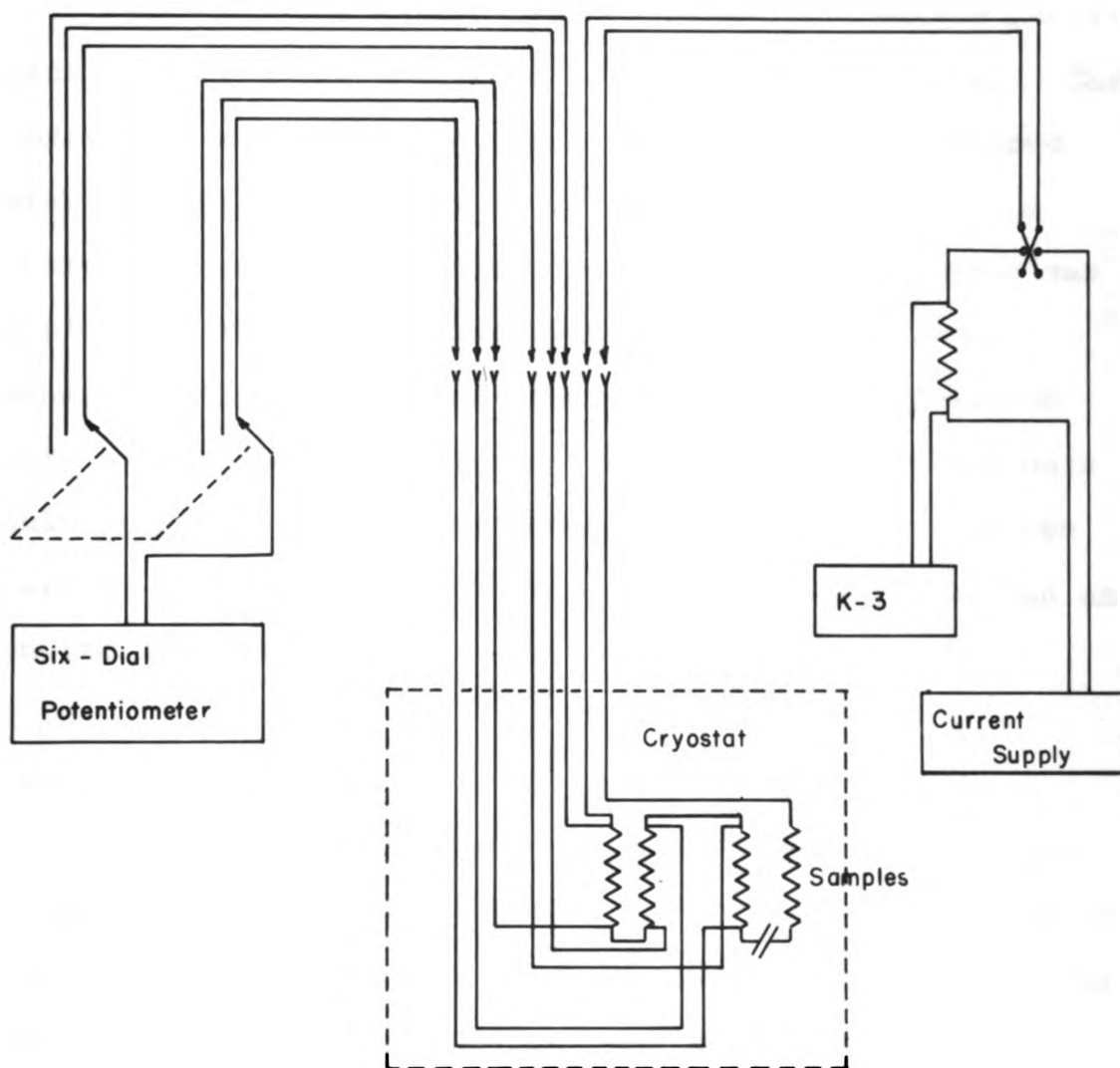
During the course of an experimental run after the temperature had stabilized at the desired value, the carbon resistance thermometer was balanced and the null detector observed throughout the course of the measurements. These observations indicated that the temperature was maintained constant to within $.0005^{\circ}\text{K}$.

Transverse magnetic fields were applied to the samples by means of a Harvey-Wells 15 inch iron core electromagnet. The dewar required a 3 inch pole tips separation. For runs III, IV, and V the magnet was equipped with 12 inch pole tips with which the maximum field was 17.7 kilogauss. For run VI, 6 inch pole tips were used with a maximum field 21.8 kilogauss. Sample lengths were less than 80% of the diameter of the pole tips and were carefully centered in the field. Measurements with a nuclear magnetic resonance probe indicated the field to be uniform to 0.5% over the sample length. During the course of the measurements the field was measured with a Rawson type 720 rotating coil flux meter. The field strength was determined to within 1%.

Electrical Measurements

The current and potential leads were brought from the thermal shielding chamber on top of the cryostat through $\frac{1}{4}$ inch copper tubing to a switch box on a shielded measuring table. The six pairs of potential leads were connected by means of a Leeds & Northrup rotary switch to a Rubicon six-dial potentiometer. Null was detected with a Guildline type

Figure 3. The Measuring Circuit



5214 photocell galvanometer amplifier operated in the series feedback mode with a sensitivity of 50 centimeters per microvolt. Noise, stability and drift were such that the resolution was approximately 2×10^{-6} volts.

The measuring current was supplied by a series parallel bank of four large lead-acid batteries (300 amp-hrs). Under constant load the current from these batteries remained stable to within one part in 10^5 . In order to vary the current a constant impedance (π - network) attenuator was employed. The current was monitored continuously by measuring the potential across a 10 ohm series resistor with a separate potentiometer (type K-3) with electronic null detector. With this arrangement a variation in the current of one part in 10^5 produced a deflection of one cm on the null detector.

Experimental Procedure

At liquid helium temperatures the first concern was to determine a proper measuring current. This was done by starting with very low currents, about 1 ma, and measuring the resistance of each sample. The current was then increased until the resistance of the smallest wire in the set showed an increase. This increase was due to the magnetoresistance produced by the self-field of the measuring current. By keeping the self-field of each sample below one gauss the resistance of the wires could be considered independent of the measuring current. A

current of 10 to 50 ma fulfilled this requirement and still produced an emf of about 5 microvolts in the larger wires. The initial decrease of resistances with increasing measuring current observed by Cochran and Yaqub (22) in single crystal gallium wires was not observed. Calculations indicated that, assuming a Hall coefficient of 0.4×10^{-15} volt-cm/amp-Oe (15), the Hall voltage across the potential contacts under the worst possible conditions could not exceed 2×10^{-8} volts. Since this is just the resolution of the experiment no corrections were made. The magnetoresistance and zero field data were obtained by fixing the temperature and the magnetic field and measuring the potential drop across each sample, first with the current in one direction and then with the current reversed to eliminate thermal emf's. The magnetic field was then changed to the next desired value and the above procedure repeated. The temperature was changed after data had been obtained for all of the desired values of magnetic field.

Recent work by Bate, Martin and Hille (23) has indicated a decrease in the resistivity of a wire as its age increases. They have attributed this to a slow recrystallization of the material after extrusion, into small crystallites whose sizes are comparable to that of the wire. To investigate this effect several samples were allowed to age at room temperature for a period of several months. Then measurements were made simultaneously on the aged wires and on wires which had been recently extruded through the same die.

Chapter IV

Presentation of Data and Discussion of Results

Four experimental runs (III through VI) were made. Runs III and IV each consisted of six samples measured in magnetic field strengths ranging from zero to 17.7 Kilo-gauss at eight temperatures between 4.2°K and 1.15°K . In run V four samples were measured at 4.2°K only. In run VI three samples were measured at fields ranging from zero to 21.2 Kilogauss at four temperatures between 4.2°K and 1.20°K . A description of these samples is contained in Table 1.

This discussion is based on the results of all of these measurements. The graphs presented show the general trend of the results as well as the deviations from those trends.

High Field Magnetoresistance

Plots of the resistivity vs. magnetic field at several temperatures are shown for 5 samples in Figures 4 to 8. These plots all display a saturation of magnetoresistance which is characteristic of indium. The degree of saturation is seen to be generally temperature dependent. There is a sharper break in the curve and a flatter plateau for lower temperature. In addition the smaller samples display a definite decrease in resistance in moderate magnetic fields. This effect is likewise temperature dependent, that is, the

TABLE I Description of Samples

<u>Designation</u>		<u>Die Size</u> (mm)	<u>d</u> (mm)	<u>1/d</u> (mm ⁻¹)	<u>Age</u> (days)
III	1	.254	.248	4.03	21
III	2	.0889	.0847	11.8	80
III	3	.0889	.0795	12.6	1
III	4	.0635	.0603	16.6	1
III	5	.0399	.0366	27.3	80
*III	6	.0229	.0189	53.0	2
IV	1	.0635	.0597	16.7	50
IV	2	.0635	.0544	18.4	4
* IV	3	.0315	.0362	27.6	50
* IV	4	.0330	.0362	30.3	4
* IV	5	.0256	.0229	39.1	3
IV	6	.0173	.0156	64.1	50
V	1	.635	.642	1.56	37
** V	2	.254	.249	4.02	300
* V	3	.0315	.0352	28.4	2
* V	6	.0229	.0185	54.4	1
VI	2	.0284	.0273	36.7	4
VI	3	.157	.159	6.29	4
VI	4	.0508	.0416	24.0	4

*Damaged dies

**This sample was taken from the same wire as III-1

$\rho \times 10^9$
(Ω -cm)

Figure 4. Resistivity vs. Magnetic Field; Sample III-1

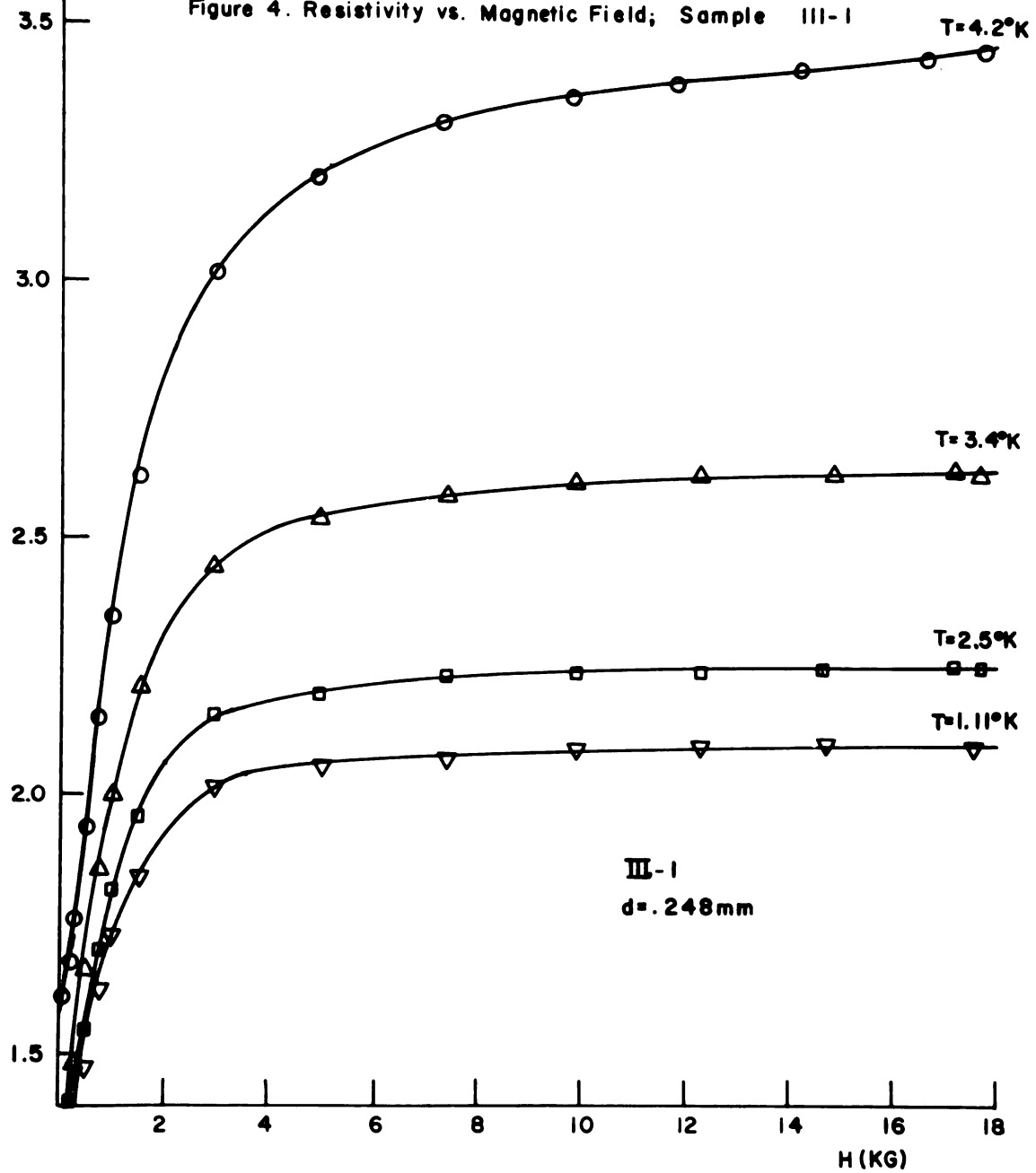
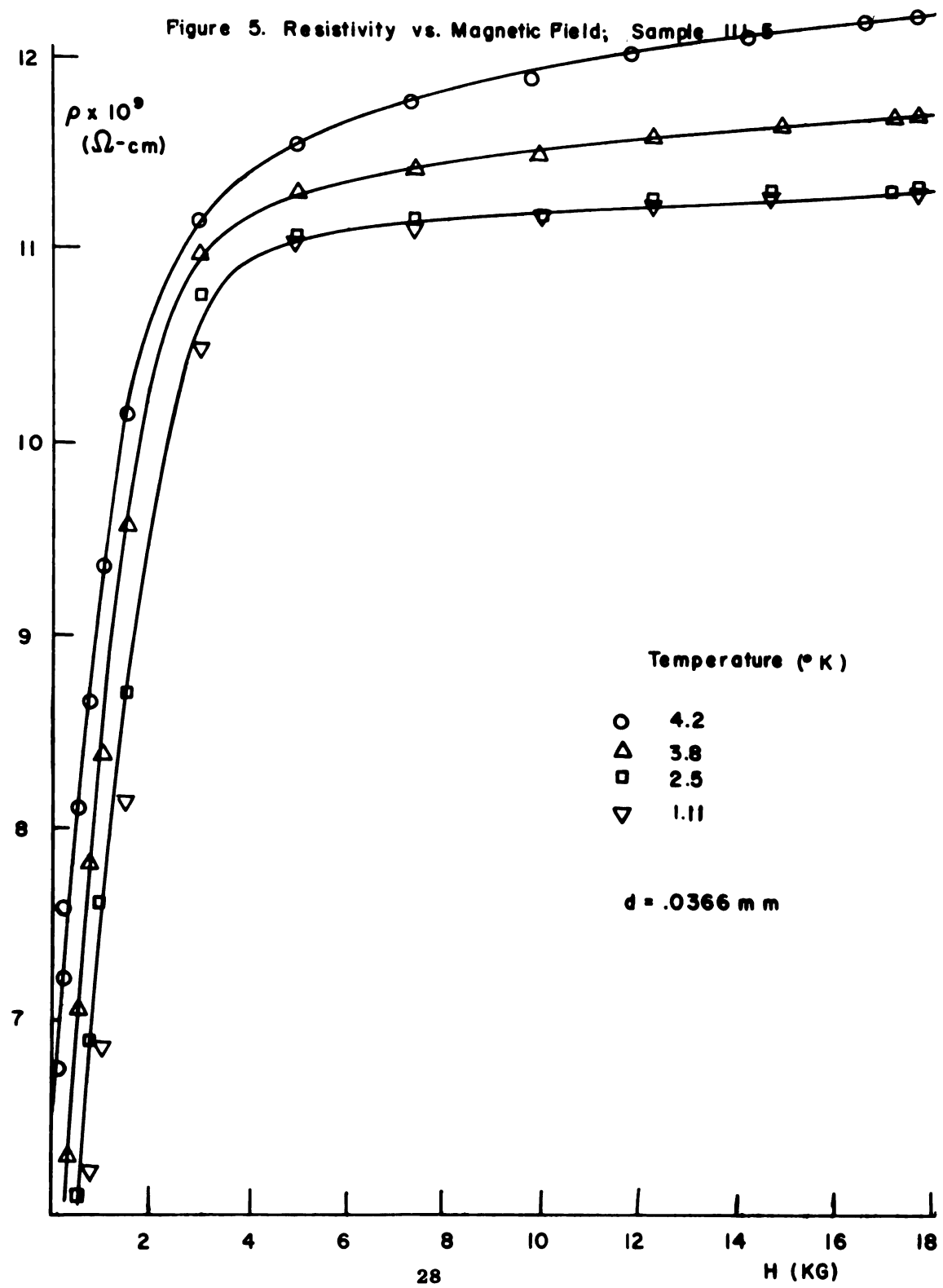


Figure 5. Resistivity vs. Magnetic Field, Sample II, 5



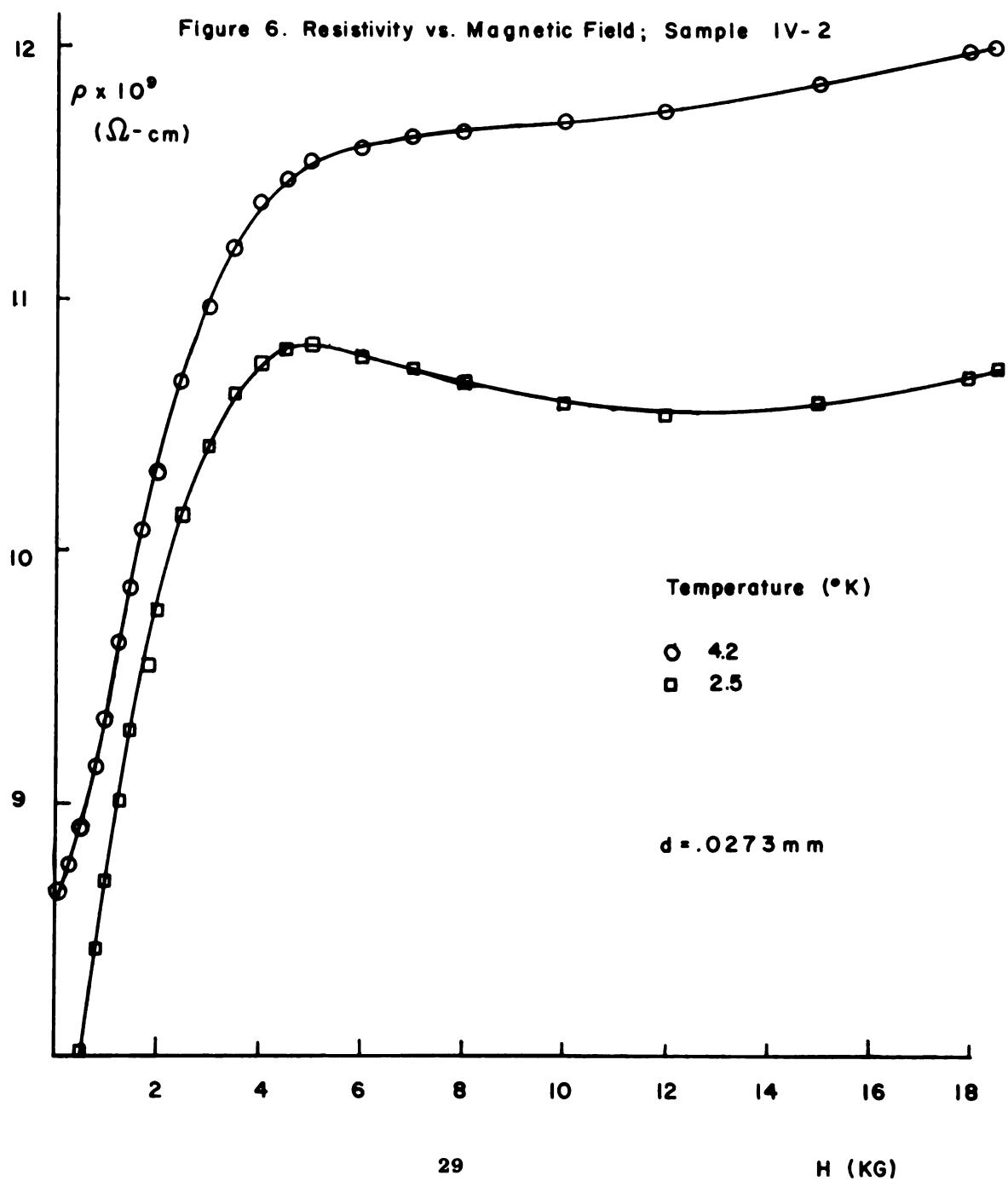


Figure 7. Resistivity vs. Magnetic Field; Sample III - 6

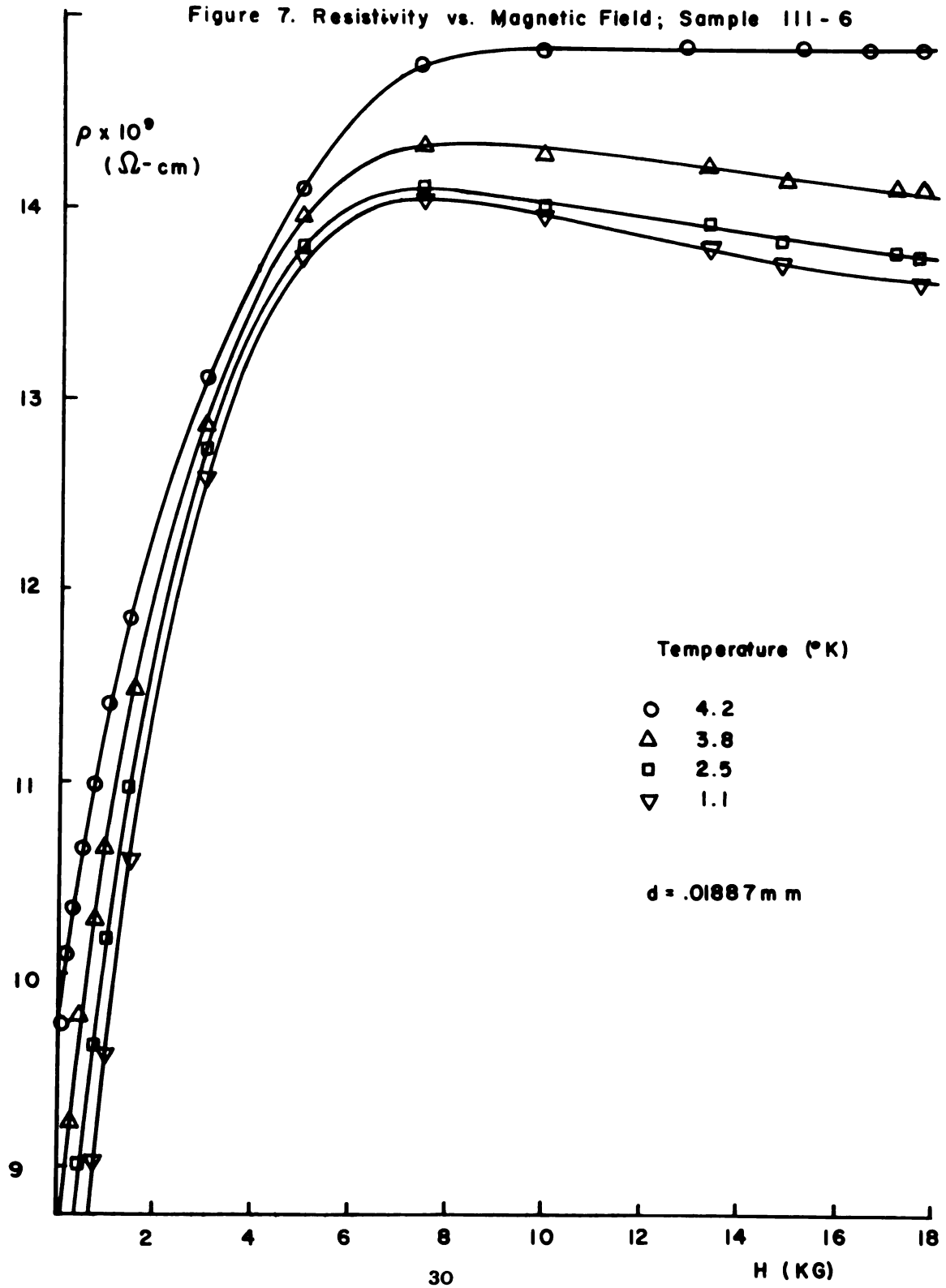
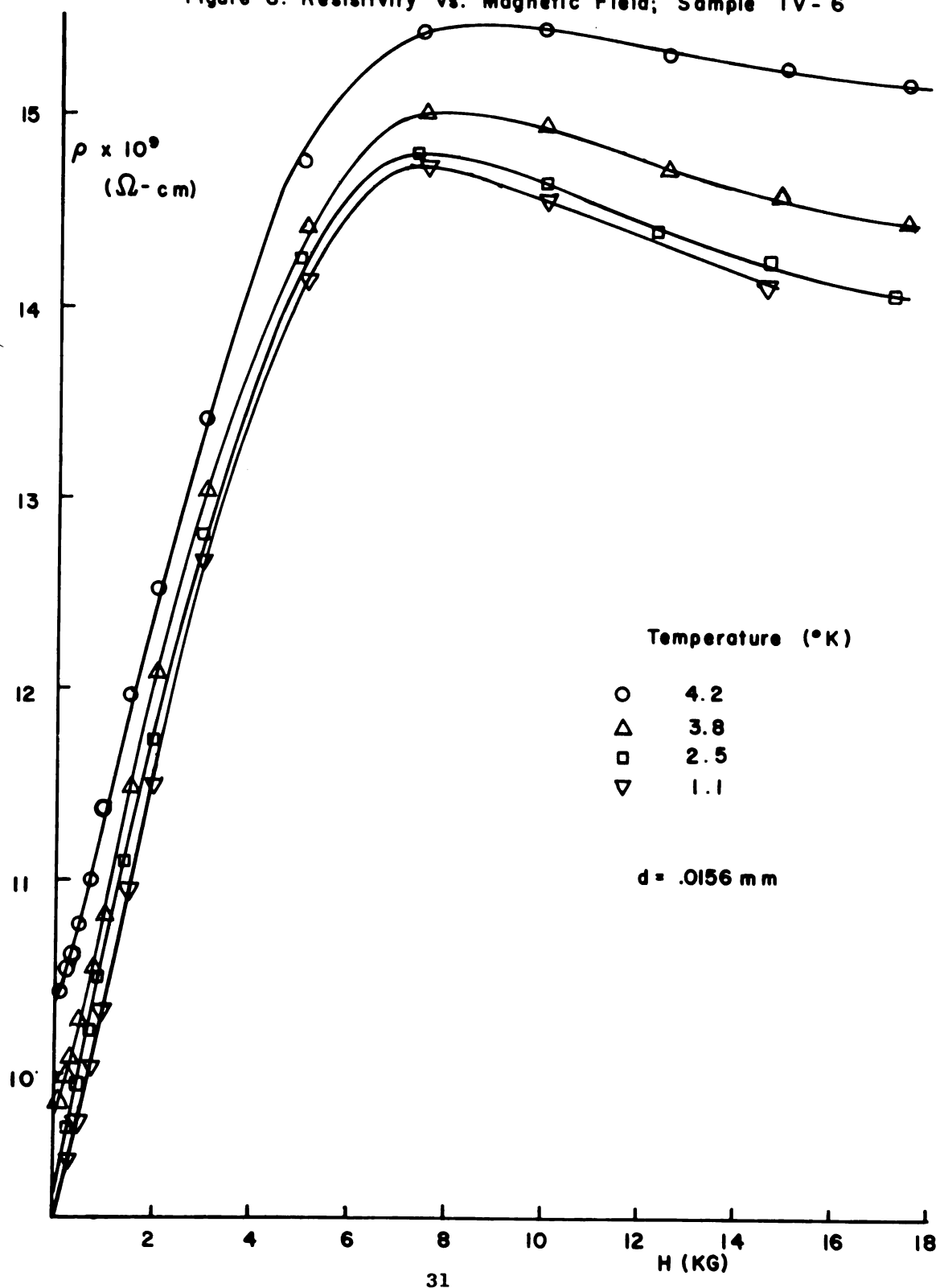


Figure 8. Resistivity vs. Magnetic Field; Sample IV-6



decrease is sharper at lower temperatures. This decrease was observed in all samples having a diameter less than .0273mm and in a few samples with diameters as large as .085mm (III-2, III-3, VI-4). This effect was not observed in any of the four samples having $d > .085\text{mm}$. In all cases when it was observed the maximum in the ρ vs. H curves was more pronounced at 1.15°K than at 4.2°K . In some cases the decrease of ρ with respect to field was observed only at the lower temperatures (Fig. 6).*

The size dependent reduction of resistivity with increasing magnetic field has previously been observed for sodium wires in a transverse field by McDonald and Sarginson (5) and for aluminum and indium films by Forsvoll and Holwech (17, 18). This effect has been ascribed by McDonald to the reduction of surface scattering of the conduction electrons when their cyclotron diameter equals the wire size that is when $r_c = \frac{d}{2}$. The fact that this effect was not observed in larger wires is not surprising since on the basis of McDonald's argument the maxima for these wires should occur in a region where the bulk magnetoresistance has not yet saturated. The effect would then be obscured by the rapid increase of the bulk resistance with magnetic field.

*In contrast to this behavior which is considered to be a real effect, several of the samples in the $d = .027\text{mm}$ range - namely samples III-5, IV-3 and IV-4 (see Fig. 5) - showed no decrease in resistance at any temperature. These samples usually displayed incomplete saturation -- that is, the resistance continued to increase slowly with increasing field beyond the 10 Kilogauss region.

If we use equation (16) and assume that the maximum in the magnetoresistance occurs at $r_c = \frac{d}{2}$, we obtain the average value of $P_f = 1.0 \pm .1 \times 10^{-19}$ gm cm/sec in fair agreement with values reported by Forsvoll from his size effect experiment (1.3×10^{-19} gm cm/sec) and in good agreement with Rayne's (24) magnetoacoustic measurements ($.83 \times 10^{-19}$ gm cm/sec). Similar results have recently been obtained for thin indium sheets by Cotti and Olsen (25). Effects of this type were observed by Olsen (7) for wires in a longitudinal field; however, he did not identify his maximum with the above orbital condition.

Low Field Magnetoresistance

Figures 9 through 12 display the resistivity of a given wire as a function of the square of the applied magnetic field in the region below 1000 gauss. These plots indicate the general deviation from the H^2 rule. Moreover, it was noted that no single exponent could be chosen which would characterize the magnetic field dependence of all samples. These changes in the field dependence do not seem to be correlated with size or age of the sample or the temperature.

Since indium becomes a superconductor below 3.39°K and since the construction of a Kohler plot requires $\rho_w(0,T)$, it is necessary to obtain values of the zero field resistivity for temperatures less than 3.39°K by indirect methods. Olsen suggested extrapolation of the ρ vs. H^2 plot to $H=0$. With

Figure 9. Resistivity vs. Magnetic Field Squared; Sample III - I

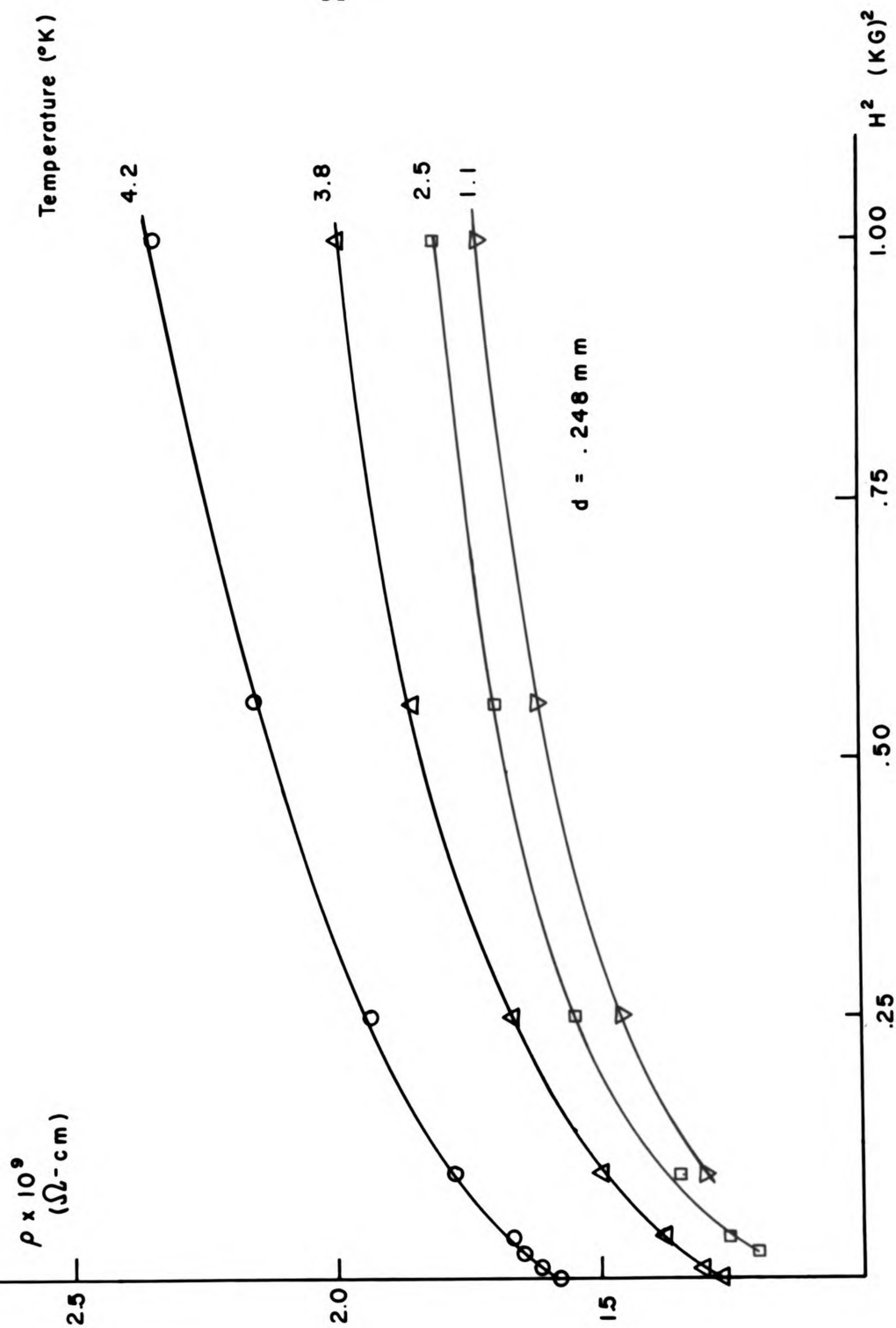
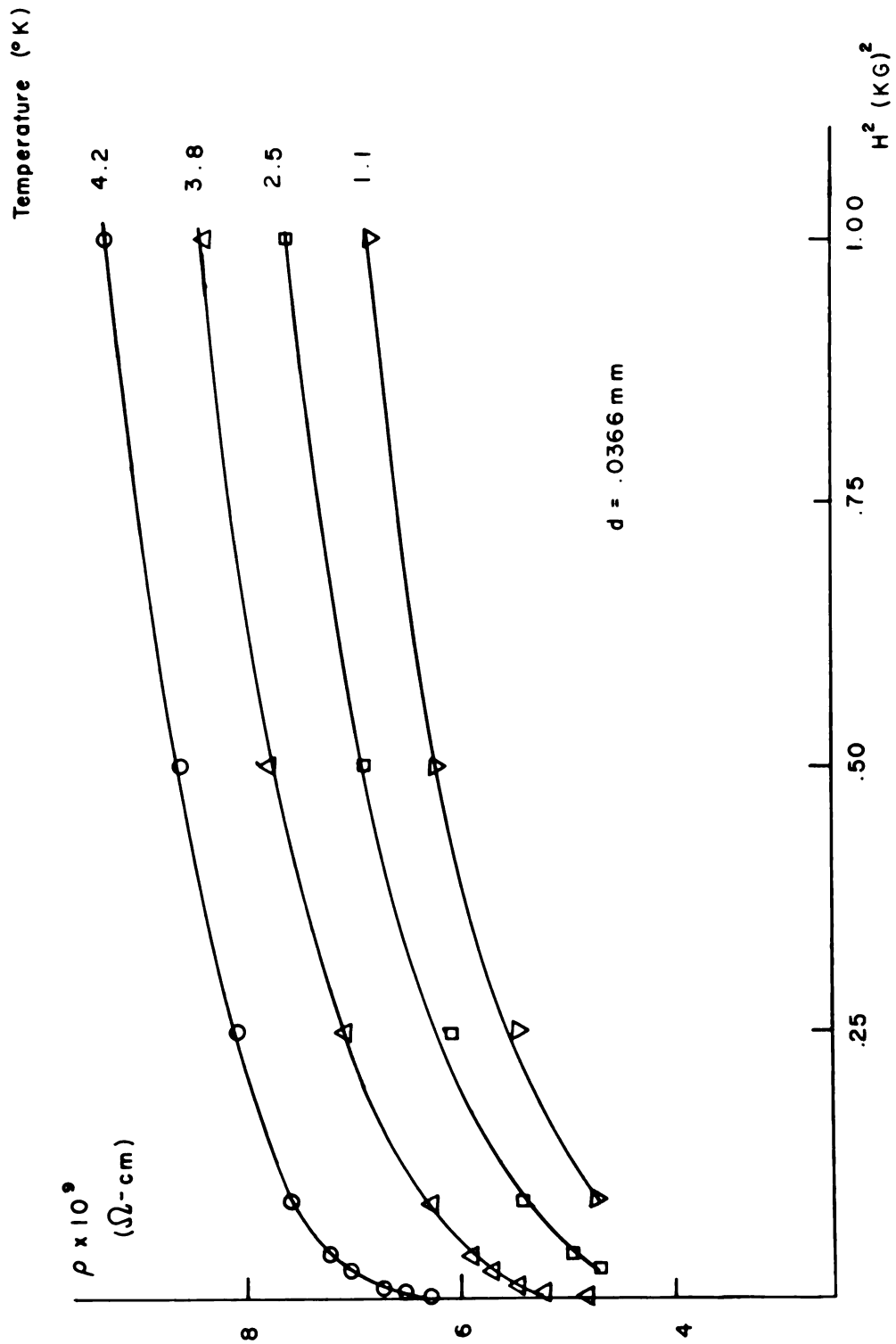


Figure 10. Resistivity vs. Magnetic Field Squared; Sample III-5



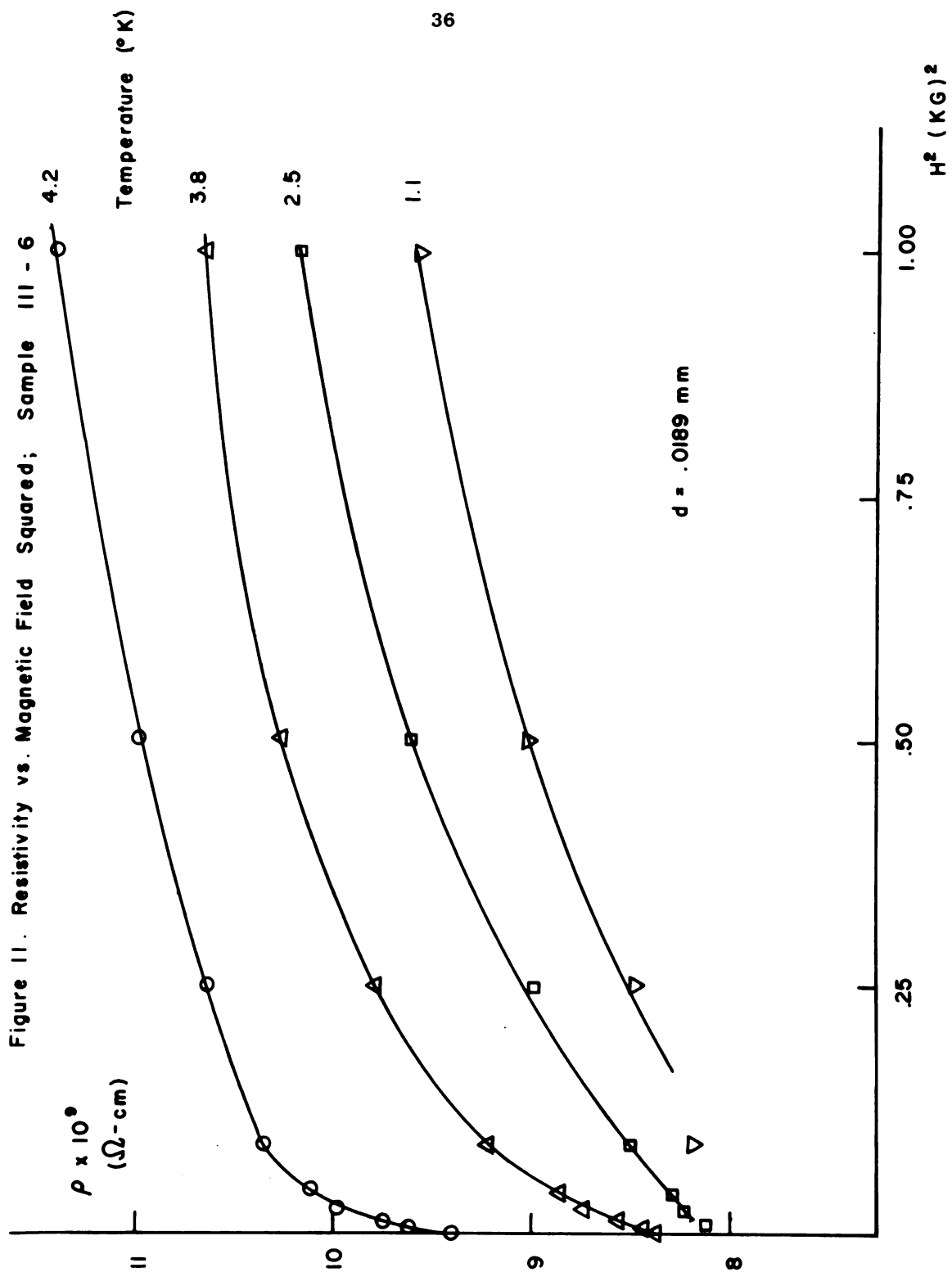
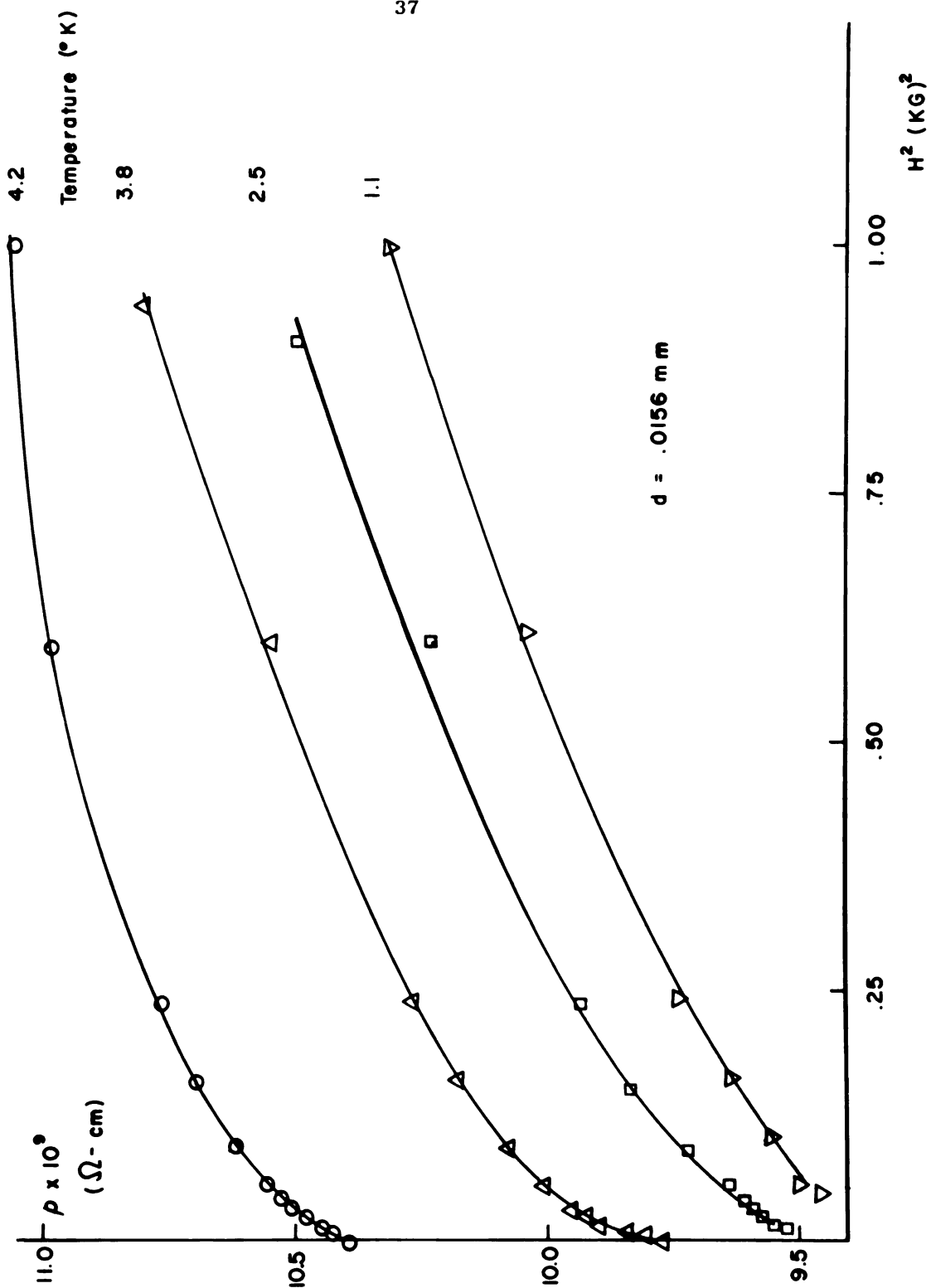


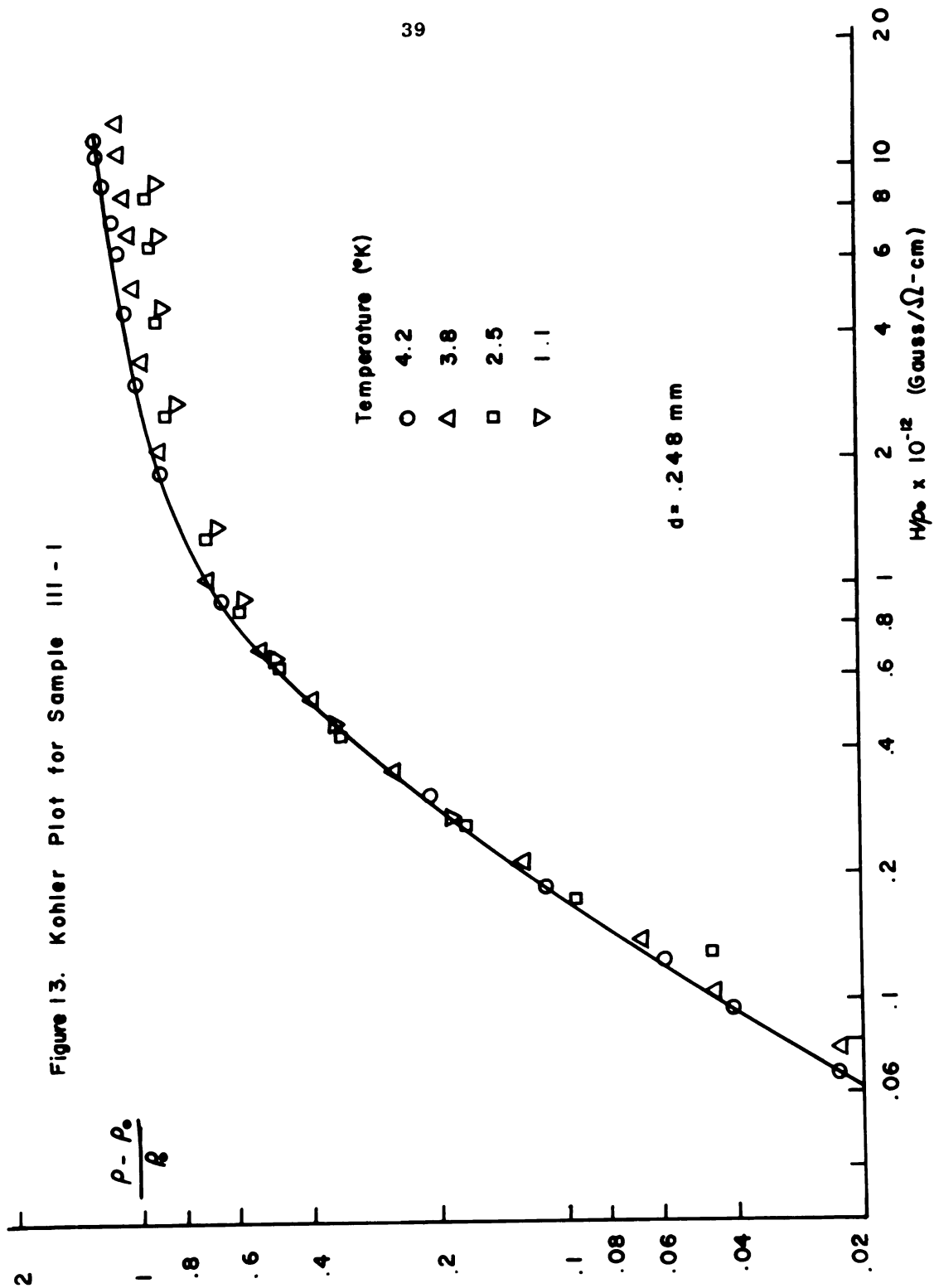
Figure 12. Resistivity vs. Magnetic Field Squared; Sample IV-6



this method of extrapolation in mind a high density of points was taken in the low field region in the present experiment. However, due to the complicated low field behavior described above, a reliable extrapolation was not possible. An extreme example of the difficulty involved here is shown in Figure 11. Another difficulty which beset this method of obtaining $\rho_w(0,T)$ was that the magnetic superconducting transition was about 50 gauss wide in some cases. This broadening made it impossible to distinguish between points which represented normal magnetoresistance and points which represented a partial superconducting state. This was an especially serious defect since the points in question were the closest ones to $H=0$ and thus should have received the greatest weighting in the extrapolation to $H=0$.

The inconsistent dependence of the magnetoresistance with respect to wire size and the broadened superconducting transition are no doubt associated with the conditions of sample preparation and the amount of impurities (especially ferromagnetic) present in each sample. As a result of these observations it was concluded that extrapolations based on this plot would be uncertain to such an extent as to invalidate the further analysis of this data.

The procedure finally used to obtain $\rho_w(0,T)$ for all samples was based on the use of Kohler diagrams (Figures 13 to 16). For $T > 3.4^\circ\text{K}$ the $\frac{\Delta\rho(H,T)}{\rho_w(0,T)}$ vs $\frac{H}{\rho_w(0,T)}$ points were computed directly from the measured values $\rho_w(0,T)$ and



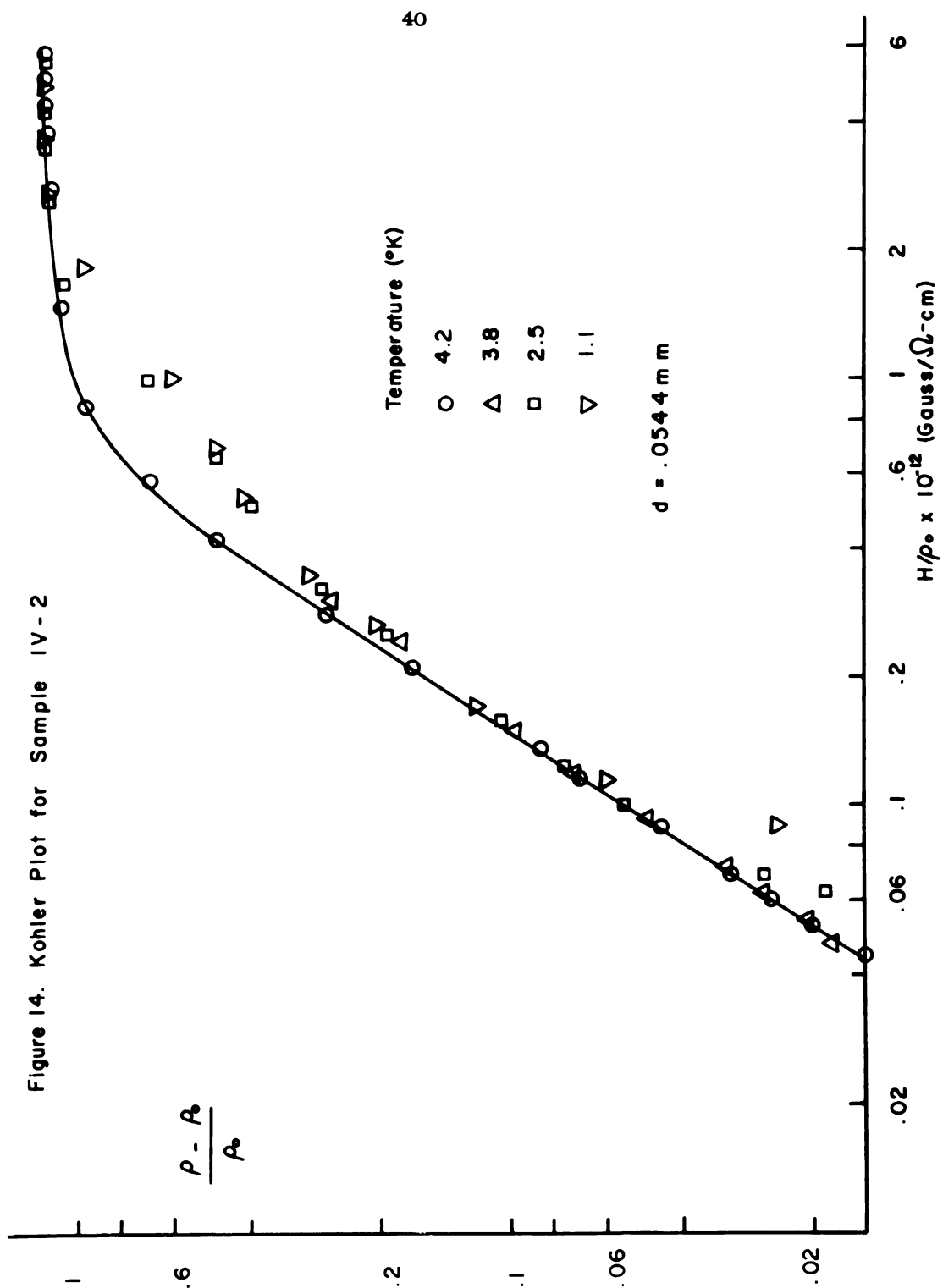


Figure 15. Kohler Plot for Sample IV-5

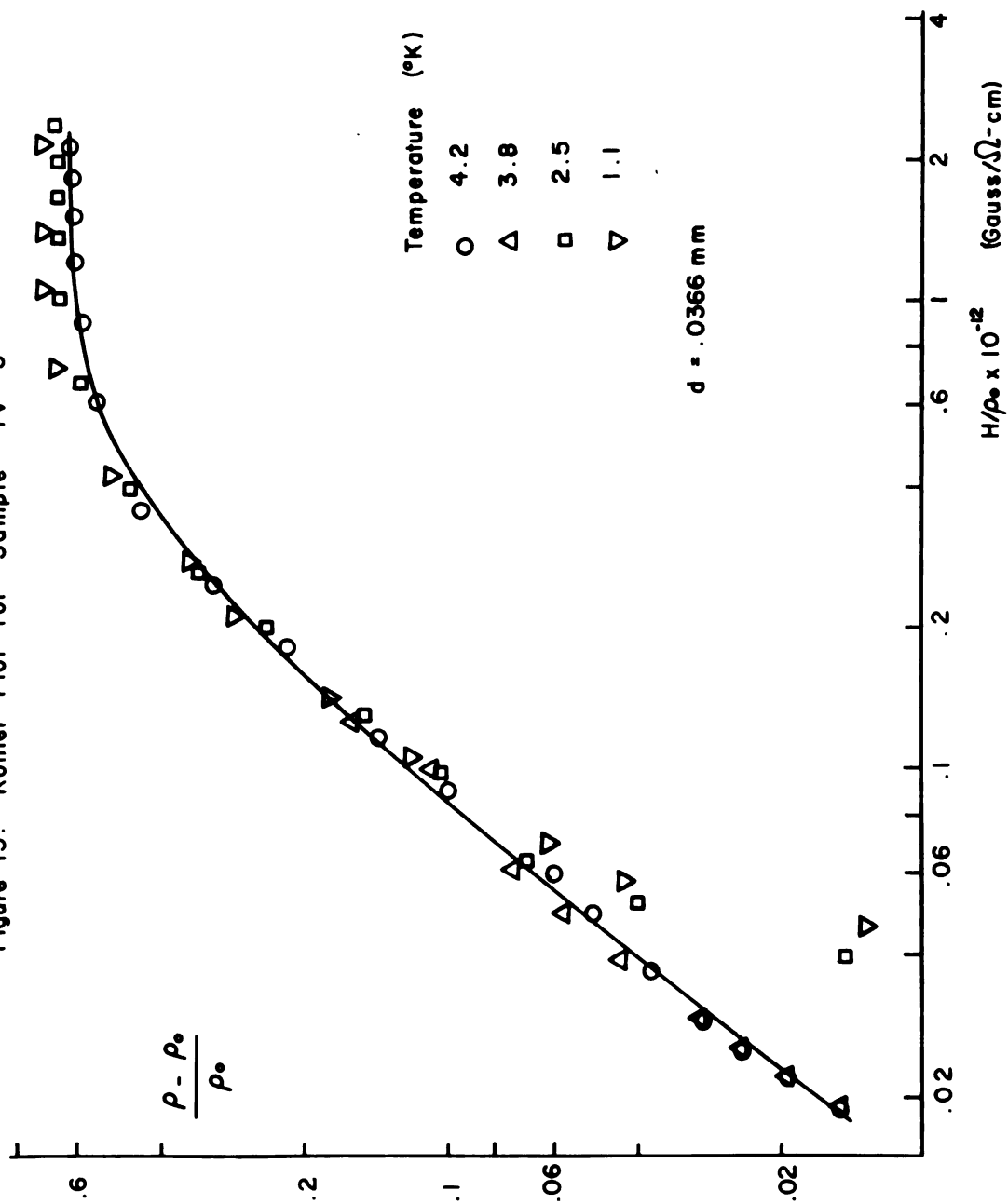
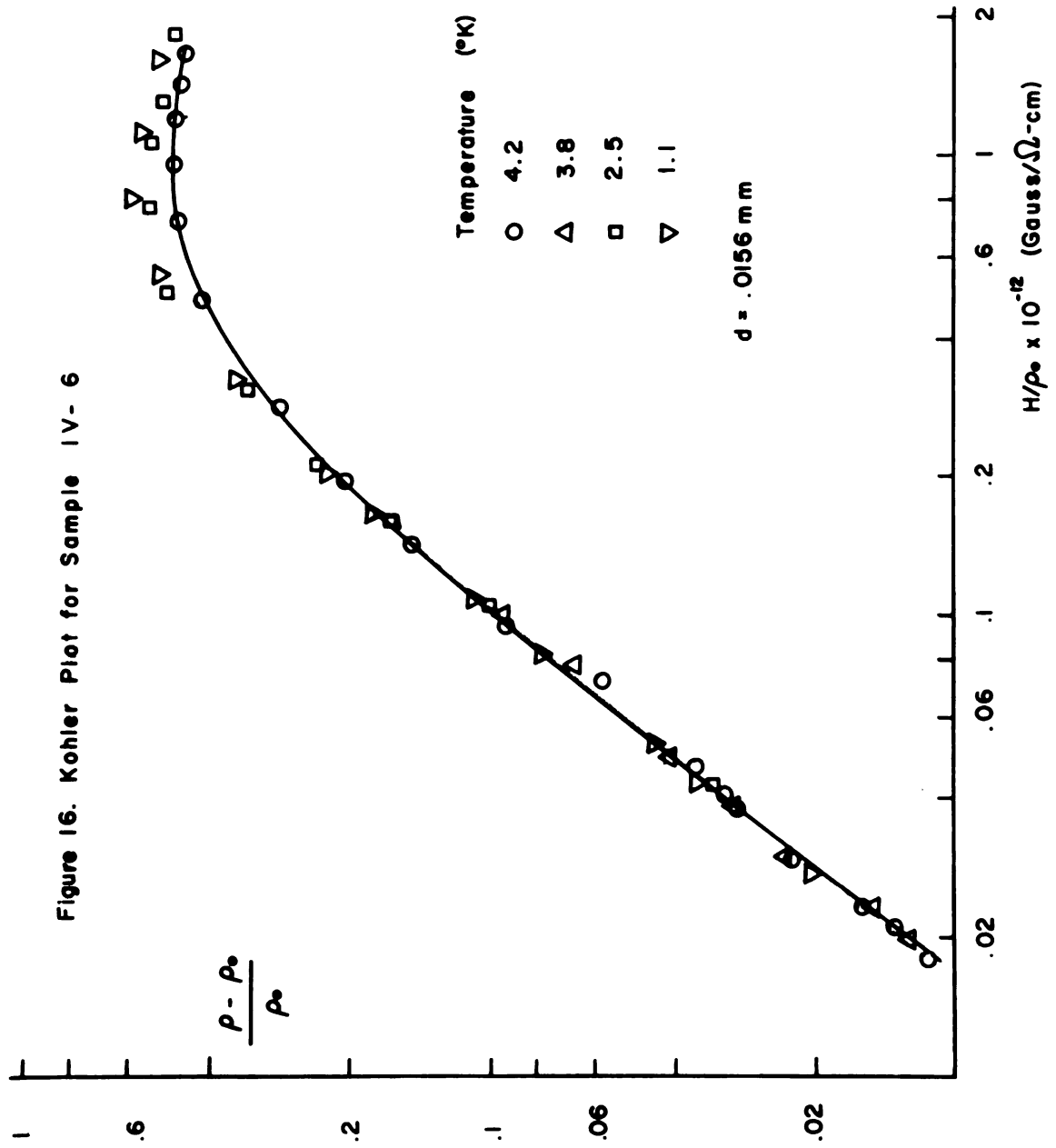


Figure 16. Kohler Plot for Sample IV-6



$\rho_w(H,T)$. The plots for these temperatures were used to define the function $f\left(\frac{H}{\rho_w(0,T)}\right)$ graphically. The function was assumed to be independent of temperature in the low field range. Here "low field" is defined to be fields corresponding to the condition $r_c > \frac{d}{2}$. The data for $T \leq 3.4^\circ\text{K}$ was fitted to this function in the low field region by adjusting $\rho_w(0,T)$. Superconducting points were easily distinguished by the fact that they could not be made to fit the function at low fields. $\rho_w(0,T)$ values obtained in this manner are presented in Table 2 and are probably not in error by more than 1% for $T > 2.0^\circ\text{K}$ and 5% for $T \leq 2.0^\circ\text{K}$.

In the saturation region of these Kohler diagrams a temperature dependent deviation from Kohler's rule is observed. For wires with $d > .08\text{mm}$ decreasing temperature produces a lower saturation value of $\frac{\Delta\rho}{\rho}$. This effect decreases as the wire size becomes smaller, vanishes for $d \approx .06\text{mm}$ (IV-1 and IV-2), and in fact, reverses for smaller diameters. The results for $d \geq .08\text{mm}$ are in qualitative agreement with those of Olsen whose smallest reported sample had $d = .10\text{mm}$. The reversal of the effect has not been previously noted. However, LaRoy's "II-7" with $d = .06\text{mm}$ seemed to show a weaker temperature dependence than did his larger samples.

This deviation at high magnetic fields for the larger wires probably has its origin in the effect proposed by Olsen. That is, in the Kohler relation the quantity ρ_w should be replaced by ρ_b since under the condition $r_c < d$

TABLE II Tabulation of Zero Magnetic Field Resistivities

Sample	d(mm)	Temperature ($^{\circ}$ K)								
		4.2	3.8	3.4	3.0	2.5	2.0	1.6	1.2	0
		Resistivity (ohm-cm $\times 10^9$)								
III-1	.248	1.582	1.413	1.277	1.190	1.145	1.105	1.096	1.089	1.085
2	.0847	3.613	3.325	3.11	2.96	2.81	2.73	2.68		2.65
3	.0795	2.669	2.476	2.34	2.23	2.17	2.13	2.08	2.058	2.05
4	.0603	3.584	3.353	3.18	3.04	2.93	2.84	2.80	2.77	2.76
5	.0366	6.301	5.89	5.51	5.18	4.83	4.57	4.35	4.28	4.24
6	.0189	9.410	8.98	8.70	8.42	8.18	7.91	7.80	7.71	7.67
IV-1	.0574	3.810	3.578	3.42	3.31	3.19	3.11	3.08	3.05	3.04
2	.0544	3.515	3.316	3.15	3.05	2.97	2.93	2.91	2.90	2.89
3	.0362	6.198	5.873	5.61	5.42	5.24	5.10	5.06	4.99	4.99
4	.033	6.727	6.39	6.13	5.93	5.72	5.60	5.54	5.51	5.48
5	.0256	8.340	8.025	7.83	7.67	7.48	7.32	7.21	7.14	7.15
6	.0156	10.388	10.097	9.87	9.70	9.52	9.41	9.36	9.31	9.30
V-1	.642	1.2067								
2	.244	1.505								
3	.0352	6.150								
6	.0185	9.996								
VI-2	.0273	8.580					7.90		7.86	7.85
3	.157	2.013	1.836				1.53		1.52	1.51
4	.0416	6.33	6.11				5.72		5.65	5.64
Bulk Resistivity Extrapolated from ρ vs. $1/d$ Plot										
ρ_b (OT)ohm-cm $\times 10^9$		0.93	0.82	0.70	0.62	0.58	0.54	0.52	0.51	0.5
l_{mfp} (mm)		0.167	0.178	0.208	0.235	0.245				0.25
$\rho_b l$ ohm-cm $^2 \times 10^{11}$		1.55	1.46	1.45	1.45					

the charge carriers generally are confined to trajectories which do not strike the surface. By using ρ_w we decrease the $\frac{\Delta\rho}{\rho}$ value for wires since $\rho_w > \rho_b$. This deviation should be more pronounced at lower temperatures where $\frac{\rho_w}{\rho_b}$ is larger.

Regarding the apparent reversal of a trend which we expect to be maintained, we note that here the low field magnetoresistance also appears to be a function of wire size itself. Our results indicate that $\frac{\Delta\rho}{\rho_w}$ at low fields increases as d is reduced. The reason for this will be described subsequently. However, it is clear that the Kohler function derived from low field data then is anomalously large, particularly for the smallest wires and lower temperatures for which this effect is greatest. It is possible that the additional magnetoresistivity mechanism operative at low fields persists to fields in excess of saturation and is responsible for the positive discrepancy.

Size Dependence of Kohler Diagrams

Figures 17 and 18 are Kohler diagrams for several samples at 4.2°K and 2.5°K respectively. In the 4.2°K plot the general features of Olsen's high field results are confirmed. The quantitative differences are probably due to differences in sample purity and preparation.

The apparent independence of Kohler's rule with respect to wire size at the lower fields suggested

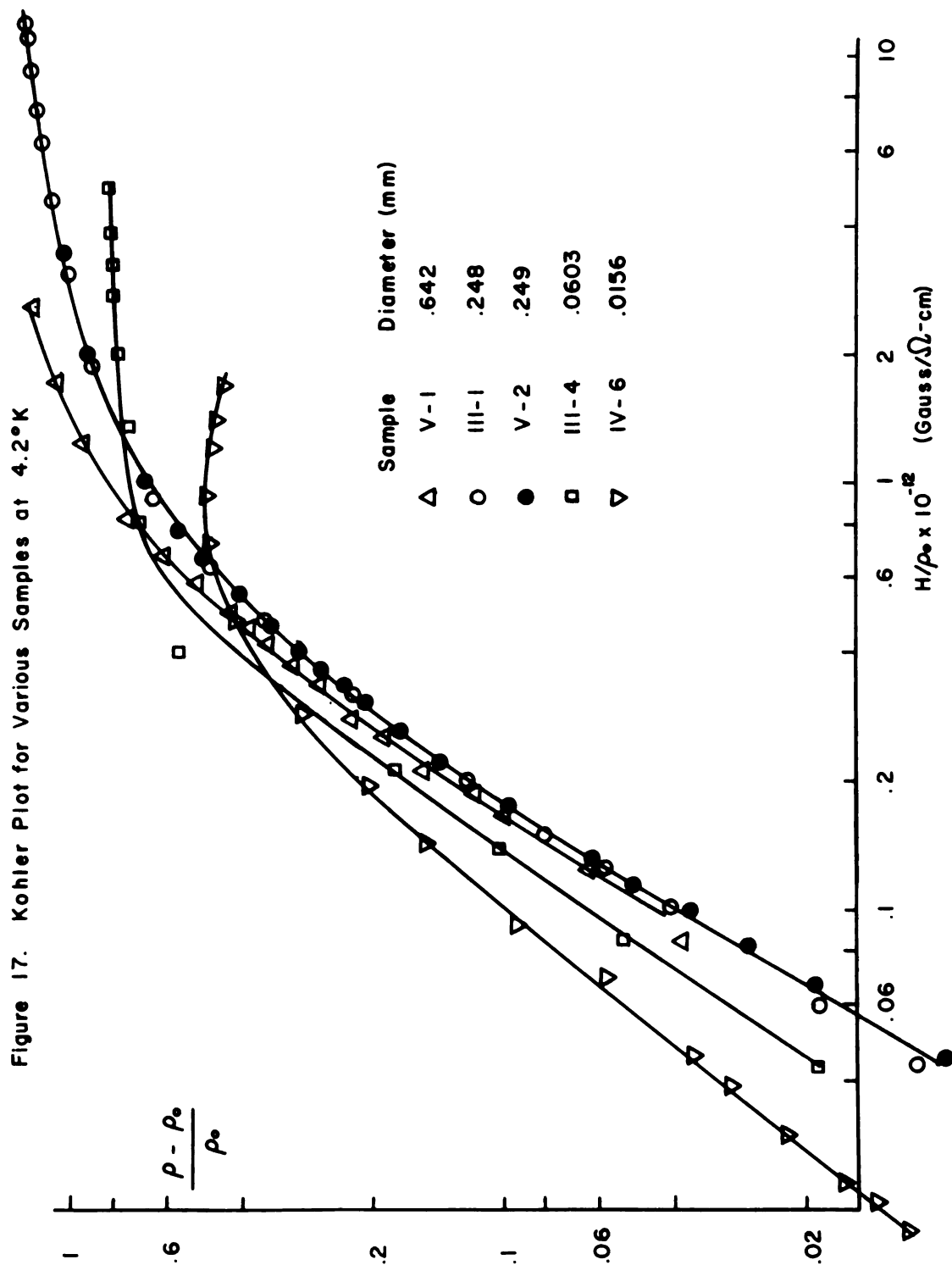
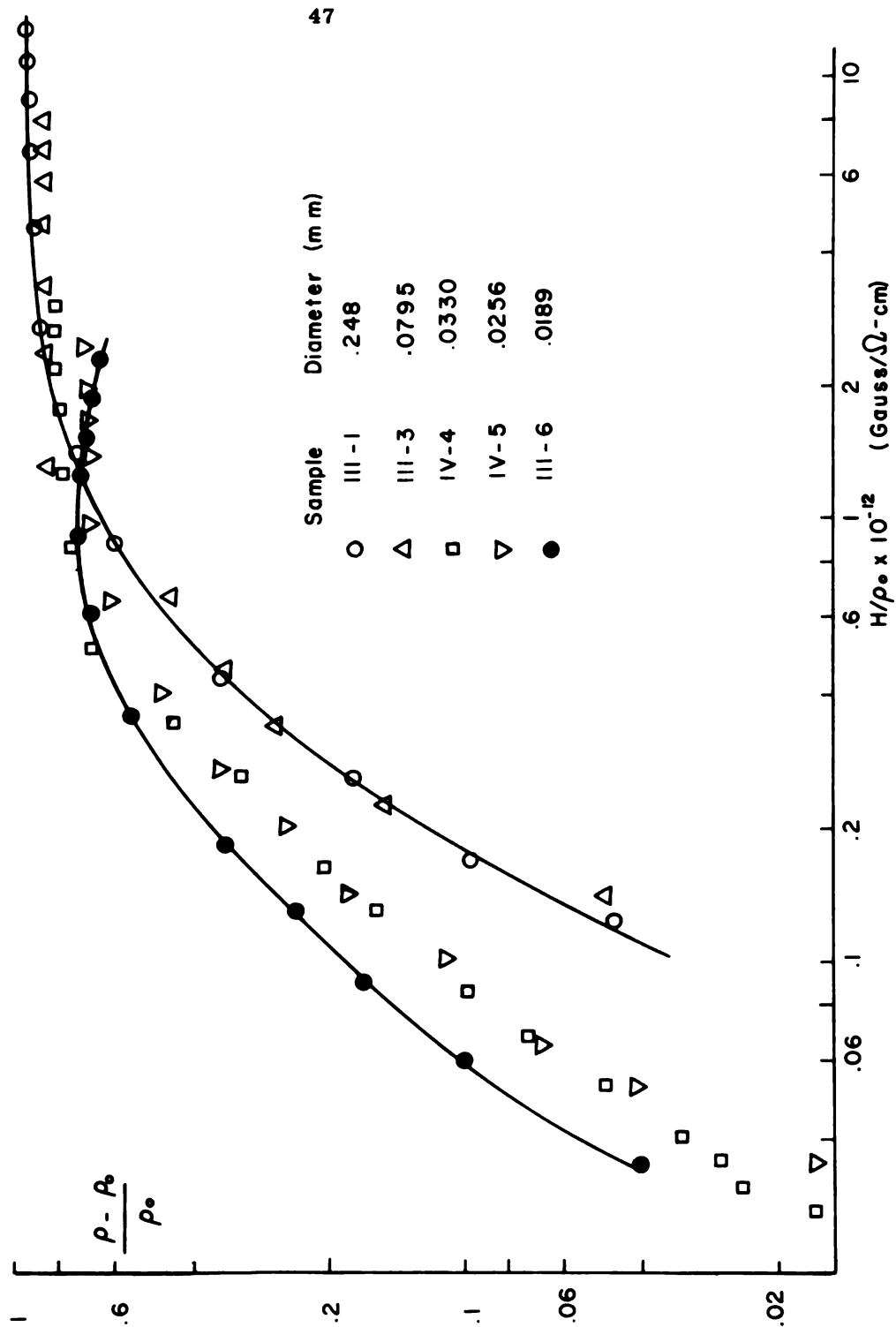


Figure 18. Kohler Plot for Various Samples at 2.5°K



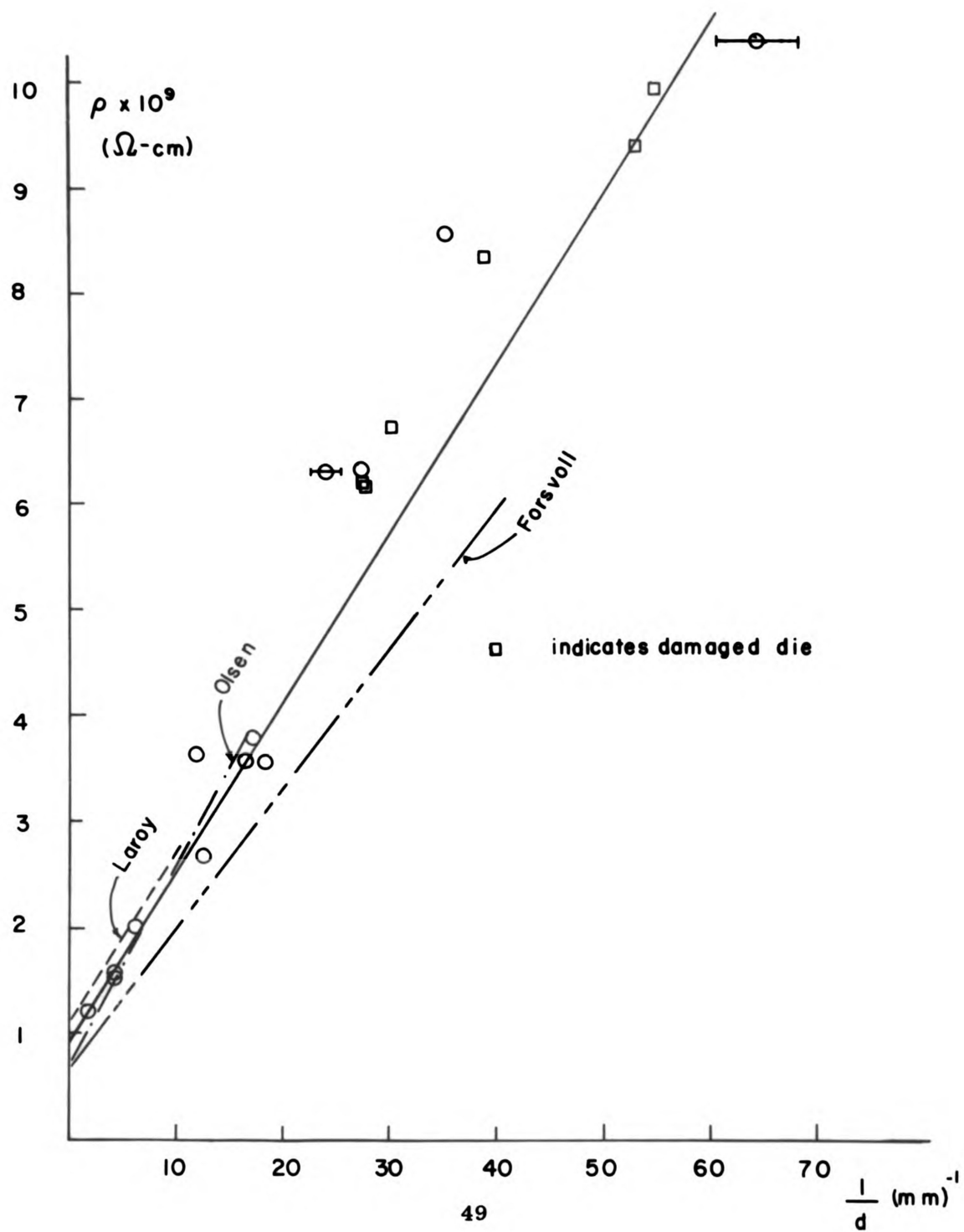
by Olsen's data, is not true for the finer wires of this study. This has also been noted by LaRoy who ascribes the increase in $\frac{\Delta\rho}{\rho}$ at low fields and decreasing wire size to an enhancement of surface scattering due to the curvature of the carrier trajectory. That is, even weak magnetic fields cause electrons which are traveling axially in the wire to follow a curved orbit to the surface, where they suffer diffuse scattering.

In both the high and low field magnetic effects the results of this experiment were not wholly self consistent. Exceptions to the high field trend are samples III-5, IV-1, 2, V-3, while some anomalous behavior occurs at low field in samples III-2, 5, IV-2, V-1, VI-2 and VI-4.

Size Effect in Zero Field -- $\frac{1}{d}$ Plot

According to the Nordheim equation a plot of $\rho_w(0,T)$ vs. $1/d$ for the various samples at a given temperature should yield a straight line with a slope of $\rho_b(0,T) \times l$ and intercept at $1/d=0$ of $\rho_b(0,T)$. $\rho_b(0,T)$ is the zero field bulk resistivity and l is the bulk mean free path at the temperature T . The data for $T = 4.2^\circ\text{K}$ is presented in this way in Figure 19. The results of several other workers are also shown for comparison. The scatter of the data points in this figure greatly exceed the 1% experimental error which can reasonably be assigned. The cause for this inconsistency is not understood at present. It should be noted, however, that subsequent to these measure-

Figure 19. Resistivity vs. Reciprocal Diameter at 4.2° K



ments the dies with which the wires had been formed were examined by the manufacturer. This examination indicated that several of the dies had been damaged. The wires which had been produced by dies which were found to be damaged are marked by an asterisk in Table I. The damage to the dies probably occurred sometime during the extrusion process wherein large pressures were exerted. Unfortunately it is impossible to tell when this damage occurred and hence all data resulting from these wires is subject to some question.

The data in figure 19 in the $1/d < 20\text{mm}^{-1}$ range indicates a linear relationship with an intercept ρ_b (bulk resistivity) = $.93 \pm .01 \times 10^{-9} \text{ ohm-cm}$ and a slope of $1.63 \pm .07 \times 10^{-11} \text{ ohm-cm}^2$. These results are in fair agreement with $\rho_b = .75 \times 10^{-9} \text{ ohm-cm}$ and $\rho_b l = 2.1 \times 10^{-11} \text{ ohm-cm}^2$ (Olsen) and to $\rho_b = .70 \times 10^{-9} \text{ ohm-cm}$ and $\rho_b l = 1.4 \times 10^{-11} \text{ ohm-cm}$ (Forsvoll and Holwech). The differences can probably again be attributed to differences in purity and sample preparation. This contention is supported by the fact that LaRoy using the same raw material and the same preparation techniques obtained results which agree closely with those found here. The lower bulk resistivity obtained by other workers indicates that either the initial purity of their material was better or that impurities and unannealed dislocations were introduced into the samples at the time of preparation.

Measurements have not been made previously in the region $1/d > 20\text{mm}^{-1}$ ($d < .10\text{mm}$). Our results suggest that the resistivity increases less rapidly in this region, a departure

from the theory of Dingle and Nordheim. This observation is, however, in disagreement with the model of Blatt and Satz according to which there should be an increase in $\Delta\rho$ for the finer wires. As will be seen below the effect depends upon temperature since for $T = 0$ the ρ vs $1/d$ graph is linear to the smaller sizes.

Values of $\rho_w(0,0)$ are tabulated in table II. The $1/d$ plot for $T = 0$ (Figure 20) is of special interest since here the Blatt and Satz phonon-surface resistivity ρ_{ps} , should not be present, leaving the slope $\rho_b l$ dependent upon the bulk material only. (For $T > 0$, l is affected by the ρ_{ps} term.) We note that

$$(\rho_b l)_{T=0} = \left(\frac{P_f}{Ne^2 l} \right) l = \frac{P_f}{Ne^2}$$

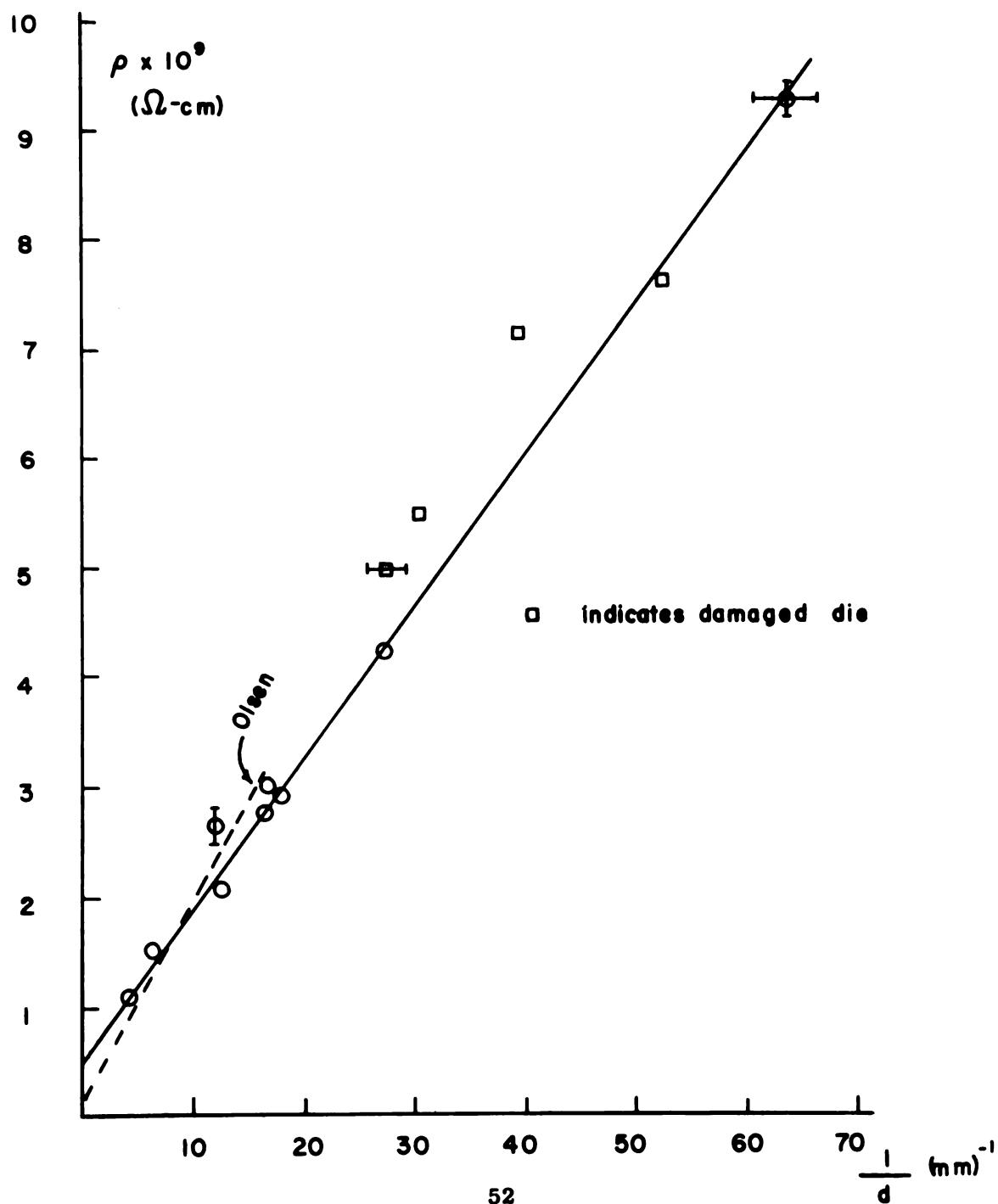
From previous information, $P_f = 10^{-19}$ gm-cm/sec and from the slope of the curve in figure 20, $\rho_b l = 1.4 \times 10^{-11}$ ohm cm². We obtain a value of 0.4 carriers per atom. The $\rho_w(0,0)$ vs $1/d$ plot also yields $\rho_b(0,0) = .50 \times 10^{-9}$ ohm-cm from which the bulk mean free path may be calculated to be $l(0,0) = .276$ mm.

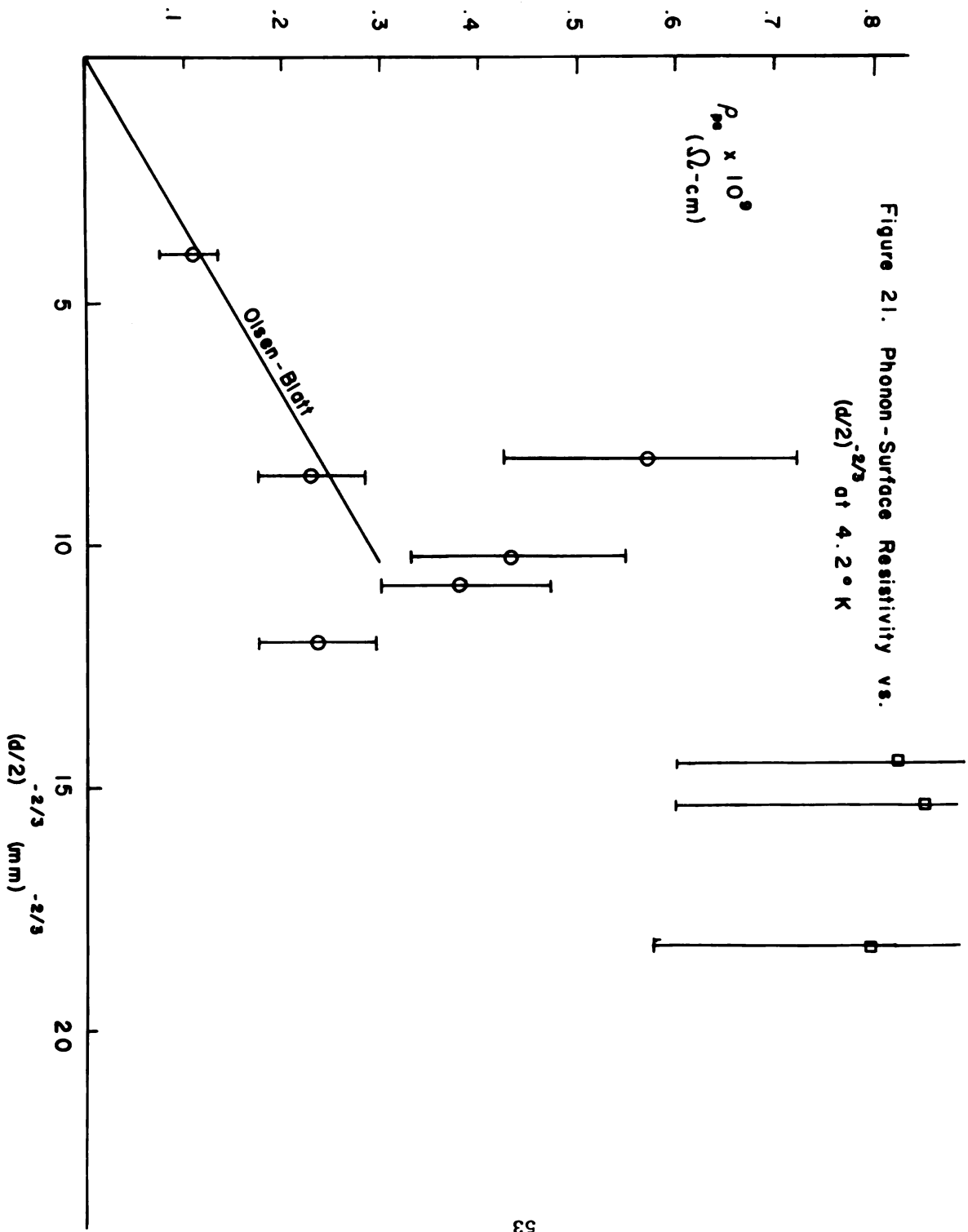
Temperature Dependent Size Effect

In order to examine the phonon-surface contribution to the total wire resistivity equation (10) can be rewritten in terms of the experimentally available values $\rho_{ps} = \rho_w(0,T) + \rho_b(0,0) - \rho_w(0,0) - \rho_b(0,T)$:

The accumulated probable experimental error here is

Figure 20. Resistivity vs. Reciprocal Diameter at 0° K





25% due, in large part, to the two fold extrapolation required to obtain $\rho_b(0,0)$ and in lesser degree to the single extrapolation to obtain both $\rho_w(0,0)$ and $\rho_b(0,T)$. Figure 21 presents $\rho_{ps}(T = 4.2)$ vs. $\left(\frac{d}{2}\right)^2$. There is here no evidence of the linear correlation predicted by Blatt and Satz; however, the large scatter in the data and lack of any systematic relationship leads one to suspect that the actual error is larger than predicted.

Chapter V

Conclusion

In this investigation the effects of transverse magnetic fields on the resistivity of thin indium wires has been studied. Previous work of this nature has produced information on wires larger than .06mm in diameter. This work extends these efforts to wires having a diameter of .0157mm. Maxima in the magnetoresistance as predicted by MacDonald and Sarginson were observed in several of the smaller wires. From the location of these maxima, a reasonable value for the momentum of electrons at the Fermi surface has been obtained.

A number of size dependent departures from Kohler's Rule were observed. For high fields ($\frac{r_c}{d} < 1$) the saturation value of $\Delta\rho/\rho_w(0,T)$ was found to decrease with decreasing wire size at 4.2°K as seen in figure 17. This observation is in good agreement with the results of Olsen within his range of sizes. The saturation values of $\Delta\rho/\rho_0$ have also been observed to be dependent upon temperature. For the larger wires the saturation value decreases as T is lowered as shown in Figure 13. This was also observed by Olsen. However for finer wires $d < .05\text{mm}$, the saturation value of $\Delta\rho/\rho_0(0,T)$ was found to increase as temperature was lowered as illustrated in Figure 16. For wires of diameter approximately equal to .05mm the effect was small or zero (Fig. 18). Turning to the low magnetic field region, departures from Kohler's rule similar to those observed by LaRoy in one case, were observed

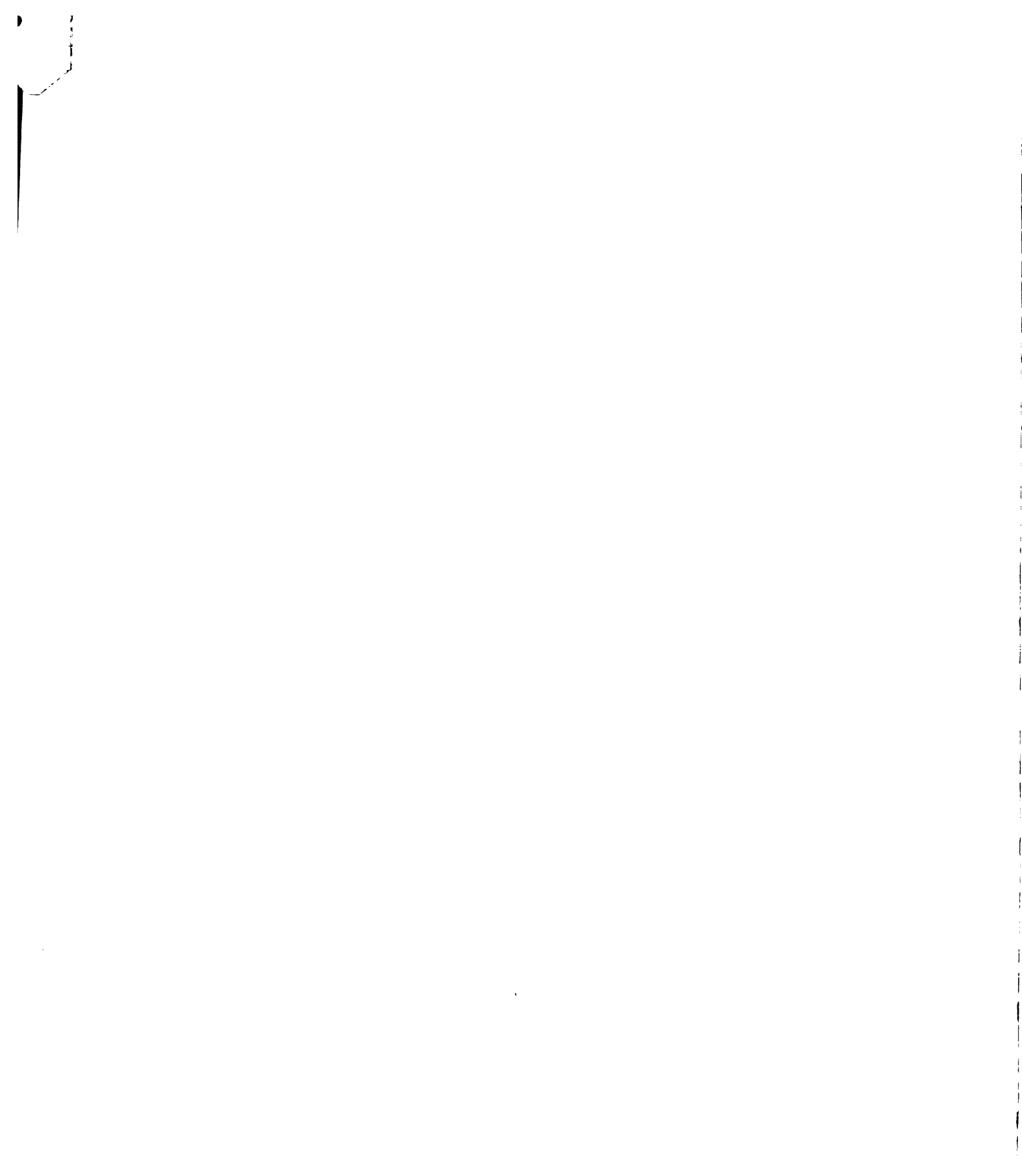
to be generally true through the entire range of samples. This effect was that at a given temperature smaller wires exhibited a larger value of $\Delta\rho/\rho(0,T)$ than did the large wires for the same value of $H/\rho(0,T)$.

The size dependence of the resistivity in zero magnetic field at $T = 0$ was found to be in good agreement with the theory of Dingle. The slope of $\rho_w(0,0)$ vs. $1/d$ plot, $\rho_b l = P_f/Ne^2 = 1.4 \times 10^{-11} \text{ ohm-cm}^2$. This result together with the value of $P_f = 1.0 \times 10^{-19} \text{ gm-cm/sec}$ gives the value of $n = 0.4$ for the number of conducting electrons per atom.

A temperature dependent size effect (departure from Mathiessens' Rule) was studied. The data shows a general qualitative trend in accord with the theory of Blatt and Satz. However, since this effect is observed only indirectly, the accumulated experimental error in this case is so large (20-50%) that no quantitative support for the theory can be claimed here.

None of the above conclusions have been found to depend upon the ages of the samples, that is the length of time that the wire annealed at room temperature. This result may indicate that the method of preparation employed produced large crystallites in the wire since other workers have observed such an age effect.

It should be emphasized that many of these results depend upon a delicate series of extrapolations. The method of analysis employed in this thesis should be verified by



measurements on a metal which has a low superconducting transition temperature, for example gallium. The method could then be applied to metals with higher transition temperatures such as lead and tin. .

In addition to the method of analysis the importance of sample preparation has also been indicated by the inconsistent behavior of a number of samples. Some of this behavior may be the result of impurities introduced during the extrusion process and some by thermal strain produced during cooling in the cryostat. For these reasons it would seem desirable to produce wire by using a nonferrous die holder for the extrusion process or by casting the sample in a plastic form. The latter would allow production of single crystal samples by seeding. The thermal strain problem may be eliminated by mounting the samples on an indium substrate.

Further information about the suspected role of impurities and crystal imperfections should be obtained by thermoelectric and thermal conductivity measurements.

Extensions of the present work in the directions of single crystals and higher magnetic fields are obvious. Single crystal studies should lead to determination of Fermi momentum and the number of effective current carriers in particular directions of \bar{k} space. High field measurements would determine the extent of the maxima observed here and may reveal oscillations in the magnetoresistances.

References

- (1) I. Stone, Phys. Rev. 6, 1 (1898)
- (2) J. J. Thomson, Proc. Camb. Phil. Soc. 11, 120 (1901)
- (3) L. Nordheim, Act. Sci. et Ind., No. 131, 1934
(Hermann Paris)
- (4) E. H. Sondheimer, Phys. Rev. 80 401, (1950)
- (5) D. K. C. MacDonald and K. Sarginson, Proc. Roy. Soc.
(London) A203, 223 (1950)
- (6) R. G. Chambers, Proc. Roy. Soc. A202, 378 (1950)
- (7) J. L. Olsen, Helv. Physica Acta 31, 713 (1958)
- (8) B. C. Laroy, Thesis for M.S. Michigan State University
(1963) Unpublished
- (9) E. H. Sondheimer, Adv. in Physics 1, 1 (1952)
- (10) E. R. Andrew, Proc. Phys. Soc. A62, (1949)
- (11) K. Fuchs, Camb. Phil. Soc. 35, 100 (1938)
- (12) R. B. Dingle, Proc. Roy. Soc. A201, 545 (1950)
- (13) F. J. Blatt and H. G. Satz, Helv. Phys. Acta 33,
1007 (1960)
- (14) Luthi and P. Wyder, Helv. Physica Acta 33, 667 (1960)
- (15) J. M. Ziman, Electrons and Phonons, Clarendon Press,
Oxford (1960), 490-492
- (16) E. H. Sondheimer and A. H. Wilson, Proc. Roy. Soc.
A190, 435 (1947)
- (17) K. Forsvoll and I. Holwech, Phil Mag 9, 435 (1964)
- (18) K. Forsvoll and I. Holwech Phil Mag 10, 181 (1964)
- (19) J. Babiskin and P. G. Siebenmann, Phys. Rev. 107,
1249 (1957)
- (20) G. K. White and S. B. Woods, R.S.I. 28, 638 (1957)
- (21) E. J. Walker, R.S.I. 30, 834 (1959)
- (22) J. F. Cochran and M. Yagub, Physics Letters 5, 307
(1963)

- (23) R. T. Bate, Bryon Martin, and P. F. Hille, Phys. Rev. 131, 1482 (1963)
- (24) J. A. Rayne, Phys. Rev. 129, 652
- (25) P. Cotti and J. L. Olsen, Cryogenics 4, 45 (1964)

MICHIGAN STATE UNIVERSITY
DEPARTMENT OF PHYSICS
EAST LANSING, MICHIGAN

MICHIGAN STATE UNIV. LIBRARIES



31293017040027